IEEE Access
Multidisciplinary ⁝ Rapid Review ⁝ Open Access Journal

Received 16 July 2023, accepted 31 July 2023, date of publication 2 August 2023, date of current version 9 August 2023.
Digital Object Identifier 10.1109/ACCESS.2023.3301144

RESEARCH ARTICLE

Observer-Based Fault Diagnosis and Fault-Tolerant Tracking Control for T-S Fuzzy Uncertain System Affected by Simultaneous Sensor and Actuator Faults

CHENGCHENG LI AND YUXIANG XIA
School of Mechatronics Engineering, Lanzhou Jiaotong University, Lanzhou 730070, China
Corresponding author: Chengcheng Li (lcc444162@126.com)

This work was supported in part by the Natural Science Foundation of Gansu Province under Grant 20JR10RA265 and Grant 20JR10RA269, in part by the Youth Natural Science Foundation of Lanzhou Jiaotong University under Grant 2020043, in part by the Tianyou Youth Talent Lift Program of Lanzhou Jiaotong University, and in part by the Higher Education Innovation Foundation of Gansu Province under Grant 2021B-112.

ABSTRACT The work presented in this article seeks to address the fault-tolerant tracking control (FTTC) problem for T-S fuzzy uncertain continuous nonlinear systems affected by sensor and actuator faults (SAFs). The T-S fuzzy model is utilized to deal with nonlinearity and uncertainty of the system. Based on a novel fuzzy observer which is constructed to estimate the values of immeasurable states and SAFs at the same time, a novel PI-type fuzzy fault-tolerant control law is mentioned to deal with the effect of SAFs simultaneously. By using Linear Matrix Inequalities (LMIs), the sufficient design conditions are converted to a convex optimization problem. The gains of reference model, observer and fault tolerant control law are obtained easily by solving the LMI conditions represented in the Theorems. The stability of the target system is ensured by applying the quadratic Lyapunov function. Finally, simulations and comparisons are given to show the validity and effectiveness of the proposed approach by two practical examples: Inverted Pendulum on a Cart and Overhead Crane System. For instance, the results presented that the tracking performance was enhanced by 23% when the faults occurred in Case 3 of Example 1, in which the comparisons are carried out with the method in Bouarar et al., (2013). The estimation error of SAFs in all cases were not exceed 2% at the steady stage of simulation.

INDEX TERMS Fault diagnosis (FD), fault-tolerant tracking control (FTTC), uncertain nonlinear systems, tracking control, sensor and actuator faults (SAFs), linear matrix inequalities (LMIs).

I. INTRODUCTION

Due to the existence of sensor and actuator faults (SAFs) or other defect within an actual system, ensuring stabilization and obtain good control performance of the system are complex and challenging issues. Therefore, in the past few years, fault diagnosis (FD) and the fault-tolerant control (FTC) for nonlinear systems have attracted a lot of attention [1], [2], [3], [4], [5], [6], [7], [8]. Many methods have been studied to address the effect of faults and the stability of the whole states. Moreover, another important work is to track arbitrarily given desired trajectories as accurately as possible. In the faulty system, finding a effective method that is able to deal with the effects of faults and also ensure good tracking performance makes the control system more challenging. Therefore, how to enhance the tracking performance of uncertain nonlinear system affected by sensor and actuator faults has been an issue of great interest and also the main motivation of the present paper.

At present, many research on FD and FTC for uncertain nonlinear systems have been carried out. Many kinds of FD observers have been widely studied, such as,

The associate editor coordinating the review of this manuscript and approving it for publication was Ming Xu.

adaptive observer [9], [10], [11], [12], [13], sliding mode observer [14], [15] and fuzzy descriptor approach [16], [17], [18], [19]. A fault estimation (FE) and a new FTC method is investigated to ensure the stability of the system affected by input signal saturation, uncertainty, external disturbances and actuator fault in [20]. In [21], a FE-based FTC method is investigated to address the stability issue for a class of nonlinear system that is affected by faults, external disturbances and sector nonlinearity in the control input. In [22], a FE-based FTC strategy were studied to guarantee the stability of system and obtain satisfactory control performance for a 3-DOF helicopter system subject to actuator drift, oscillation fault and input saturation. A fault-tolerant tracking control(FTTC) scheme for a discrete-time T-S fuzzy nonlinear systems only affected by actuator fault is investigated to ensure the stability and achieve desired tracking performance in [23]. In these literatures, a single fault is only considered in the close-lop systems or the faults are estimated in way of separation. Whereas, SAFs of a system always coexist and occur within the same time in many practical applications so that the two different system faults may not be diagnosed which can degrade the performance, increase maintenance cost and reduce production efficiency. So, how to design an valid observer to estimate SAFs simultaneously is an important issue.

Actually, from the following recent works, it can be seen that FTC approach for T-S fuzzy uncertain systems affected by SAFs has not been completely studied. Authors in [24] proposed an integral slide mode based control method to address the cooperative tracking problem for a class of nonlinear systems with uncertainties, actuator faults and external disturbances. However, only a specific kind of external disturbance is considered and the chattering problem is not fully settled. In [25], the states and actuator faults of doubly fed induction generators are estimated by a PI-type observer, but the actuator faults are regard as a bound signal which limits this method to be spread and applied. In [26], an adaptive sliding mode approach is proposed for a class of uncertain fractional-order nonlinear systems which affected by actuator faults and external disturbances to address the stability and tracking problem. However, the sensor fault has not been considered during the design process. Indeed, in [27], authors have studied the adaptive fuzzy FTC method with unknown control directions for a class of multi-input multi-output (MIMO) uncertain nonlinear systems under the condition of existence of time-varying asymmetric output constraints, but only sensor faults are paid close attention to. In fact, compared with single fault issue, the compensation of multiple faults for a real system is more general and complex. In [28], authors considered a kind of FTC method for a dynamic nonlinear systems affected by both known and unknown inputs to address the problem of SAFs estimation, but only slow-varying fault signal is applied in the systems. Both SAFs are compensated by an observer based FTC scheme in [29]. Authors in [30], [31], and [32] have also studied a series of FTC methods for systems affected by SAFs to deal with the stability problem. However, the tracking problem is not considered in these works.

In order to solve the problems mentioned above, motivated by [23] and [32], authors in this article have investigated an observer-based FD and FTTC method for a class of T-S fuzzy nonlinear systems subject to uncertainties and SAFs. The T-S fuzzy model is applied to approximate the system nonlinearity as accurate as possible. The states and faults are assumed to be immeasurable that estimated by the proposed novel fuzzy observer at the same time. Furthermore, a fault-free system is regarded as a standard reference model by which the tracking control law is designed. A new PI type fuzzy FTTC scheme is proposed to deal with the effect of SAFs and track the desired trajectories.

To sum up, the main contribution of the article is show as follows:

1) A novel fuzzy observer is investigated to address the problem of SAFs estimation for uncertain nonlinear system. Whereas, only sensor fault [33], [34] or actuator fault [35], [36] is considered in many researches.

2) A new PI type fuzzy FTTC scheme is proposed to deal with the effect of SAFs simultaneously and track the desired trajectories which is more complex and challenging than no tracking issue as [33] and [37].

3) The tracking problem is addressed with more complex actuator faults such as exponential actuator fault and time varying actuator fault. Whereas, in many researches [38], [39], [40], [41], only the constant actuator fault is studied.

The paper is organized as follows: Section II introduces a class of T-S fuzzy uncertain system affected by sensor and actuator faults. In Section III, the main results of the mentioned scheme are designed including three contents: fault-free case, post-fault case and novel FTC method. Two practical examples are used in Section IV to explain the validity of the mentioned approach. Finally, some conclusions are provided in Section V.

II. PROBLEM FORMULATION

Generally speaking, most of the actual systems are affected by faults and uncertainties. Thus, these malfunctions should be considered in one unified framework that is more helpful for popularization and application. The following T-S fuzzy uncertain system subject to SAFs with r rules is considered:

IF Rule i: $\xi_1(t)$ is$M_{1i}$and $\cdots$ and$\xi_p(t)$ isM_{pi}

Then

$$\begin{cases} \dot{x}_{f_1}(t) = (A_{11}^i + \Delta A_{11}^i)x_{f_1}(t) + (A_{12}^i \\ +\Delta A_{12}^i)x_{f_2}(t) \\ \dot{x}_{f_2}(t) = (A_{21}^i + \Delta A_{21}^i)x_{f_1}(t) + (A_{22}^i + \Delta A_{22}^i)x_{f_2}(t) \\ +B_i u_f(t) + F_i f_a(t) \\ y_f = C_i \begin{bmatrix} x_{f_1}(t) \\ x_{f_2}(t) \end{bmatrix} + E_i f_s(t) \end{cases}$$

where $x_f = [x_{f_1}(t), x_{f_2}(t)]^T \in R^n$ is the state vector of the faulty system, $u_f(t)$ represents the control input signal, y_f is the output of the system that assumed be measured in this article. F_i and E_i are constant real matrices. $f_a(t) \in R^r, f_s(t) \in R^r$ represent sensor and actuator fault. $\xi(t) = [\xi_1(t), \cdots, \xi_p(t)]$ are the premise variables assumed to be measurable; M_{pi} are the corresponding fuzzy sets. $h_i(\xi(t)) = w_i(\xi(t))/\sum_i^r w_i(\xi(t))$ with $w_i(\xi(t)) = \prod_{j=1}^p M_{ji}$. It is noted that $\sum_{i=1}^r h_i(\xi(t)) = 1$ for all $t > 0$ are the normalized weights, where $h_i(\xi(t)) \geq 0$, for$i = 1, \cdots, r$.

By using a standard singleton fuzzifier, fuzzy inference and weighted defuzzifier, the uncertain nonlinear system is presented as the following equivalent T-S fuzzy model:

$$\begin{cases} \dot{x}_f(t) = \sum_{j=1}^r h_i(\xi(t)) \left[\bar{A}_i x_f(t) + \bar{B}_i u_f(t) + \bar{F}_i f_a(t)\right] \\ y_f(t) = \sum_{i=1}^r h_i(\xi(t)) \left[C_i x_f(t) + E_i f_s(t)\right] \end{cases} \tag{1}$$

where

$$A_i = \begin{bmatrix} A_{11}^i & A_{12}^i \\ A_{21}^i & A_{22}^i \end{bmatrix}, \Delta A_i = \begin{bmatrix} \Delta A_{11}^i & \Delta A_{12}^i \\ \Delta A_{21}^i & \Delta A_{22}^i \end{bmatrix},$$

$$\bar{B}_i = \begin{bmatrix} 0 \\ B_i \end{bmatrix}, \bar{F}_i = \begin{bmatrix} 0 \\ F_i \end{bmatrix}, \bar{A}_i = A_i + \Delta A_i, C_i = I_p$$

We defined the uncertainties of the fuzzy system as the Lebesgue measurable form: $\Delta A_i = H \Delta a E_a$ to describe the system uncertainties with time-varying parameter. H and E_a are specific constant matrices with appropriate dimensions. $\Delta a(t)$ represents a kind of unknown but bounded time-varying matrix functions that contain Lebesgue measurable elements. Furthermore, the classical bounded conditions $\Delta a(t)^T \Delta a(t) \leq I, \forall t > 0$ is satisfied.

Assumption 1: We assume that the matrix B_i is full column rank so that the corresponding matrix $B_i^T B_i$ is invertible.

Assumption 2: For fault f_a and f_s, the condition is satisfied $\|f_s\| \leq \bar{f}_s$, $\|f_a\| \leq \bar{f}_a$ with unknown positive scalars $\bar{f}_s, \bar{f}_a$, respectively. Moreover, f_a and f_a have norm-bounded first time derivatives

Remark 1: The type of model in Eq. (1) has been extensively used in nonlinear control, filtering and stability analysis and can be always used to describe a class of actual systems, such as missile system, servomotor system, a mass-spring-damper system, a three-tank system, and chaotic system and so on.

III. MAIN RESULTS

To find the main results, the following lemmas have been used in this article.

Lemma 1 ([42]): For the matrices X, Y, and positive constant α, the next inequalities satisfy:

$$X^T Y + Y^T X \leq \alpha X^T X + \alpha^{-1} Y^T Y$$

Lemma 2: [43] (**Schur's complement**). For the following symmetric matrix:

$$S = \begin{bmatrix} S_{11} & S_{12} \\ S_{12}^T & S_{22} \end{bmatrix}$$

the next inequalities are equivalent:

(i) $S < 0$; (ii) $S_{22} < 0, S_{11} - S_{12} S_{22}^{-1} S_{12}^T < 0$;
(iii) $S_{11} < 0, S_{22} - S_{12}^T S_{11}^{-1} S_{12} < 0$;

A. FAULT-FREE CASE

In this case, $f_a(t) = f_s(t) = 0$ satisfied, $u_f(t)$ is replaced by $u(t)$. The faulty system (1) can be expressed as a reference model:

$$\begin{cases} \dot{x}(t) = \sum_{j=1}^r h_i(\xi(t)) \left[\bar{A}_i x(t) + \bar{B}_i u(t)\right] \\ y(t) = \sum_{i=1}^r h_i(\xi(t)) C_i x(t) \end{cases} \tag{2}$$

Then, the desired state vector is defined as $x_d = [x_{1d}^T x_{2d}^T]^T$, the error vector is $e(t) = [e_1(t)^T e_2(t)^T]^T$, where $e_i(t) = x_{f_i}(t) - x_{id}(t), i = 1, 2$. The corresponding error system is given as:

$$\begin{cases} \dot{e}_1(t) = \left(A_{11}^i + \Delta A_{11}^i\right) e_1(t) + \left(A_{12}^i + \Delta A_{12}^i\right) e_2(t) + \vartheta_1 \\ \dot{e}_2(t) = \left(A_{21}^i + \Delta A_{21}^i\right) e_1(t) + \left(A_{22}^i + \Delta A_{22}^i\right) e_2(t) \\ +B_i u(t) + \vartheta_2 \end{cases} \tag{3}$$

where $\vartheta_1(t) = \left(A_{11}^i + \Delta A_{11}^i\right) x_{1d} + \left(A_{12}^i + \Delta A_{12}^i\right) x_{2d} - \dot{x}_{1d}, \vartheta_2(t) = \left(A_{21}^i + \Delta A_{21}^i\right) x_{1d} + \left(A_{22}^i + \Delta A_{22}^i\right) x_{2d} - \dot{x}_{2d}$.

We define $\bar{A}_{11} = \left(A_{11}^i + \Delta A_{11}^i\right), \bar{A}_{12} = \left(A_{12}^i + \Delta A_{12}^i\right)$, $\bar{A}_{21} = \left(A_{21}^i + \Delta A_{21}^i\right), \bar{A}_{22} = \left(A_{22}^i + \Delta A_{22}^i\right)$, Eq. (3) can be rewritten as:

$$\begin{cases} \dot{e}_1(t) = \bar{A}_{11} e_1(t) + \bar{A}_{12} e_2(t) + \vartheta_1 \\ \dot{e}_2(t) = \bar{A}_{21} e_1(t) + \bar{A}_{22} e_2(t) + B_i u(t) + \vartheta_2 \end{cases} \tag{4}$$

Now, we consider the follow PDC control law:

$$u(t) = K_{\vartheta_i} \vartheta_2(t) + K_{h_i} e(t) \tag{5}$$

where $K_{\vartheta_i} = -(B_i{}^T B_i)^{-1} B_i^T$, By combining the control law (5) with Eq. (4), the next closed-loop error model is obtained:

$$\begin{aligned} \dot{e}(t) &= \begin{bmatrix} \bar{A}_{11} & \bar{A}_{12} \\ \bar{A}_{21} & \bar{A}_{22} \end{bmatrix} e(t) + \begin{bmatrix} 0 \\ B_i \end{bmatrix} K_{h_i} e(t) + \begin{bmatrix} I \\ 0 \end{bmatrix} \vartheta_1 \\ &= \left(\bar{A}_i + \bar{B}_i K_{h_i}\right) e(t) + \bar{I} \vartheta_1 \\ &= A_e e(t) + \bar{I} \vartheta_1 \end{aligned} \tag{6}$$

where $K_{h_i} = [K_{e_1}, K_{e_2}]$

The attenuation of the tracking error for desired trajectory signal can be ensured by using the H_∞ criterion with regard to the disturbance error ϑ_1 as:

$$\int_0^{t_f} e(t)^T Q e(t) dt \leq \gamma^2 \int_0^{t_f} \vartheta_1(t)^T \vartheta_1(t) dt \tag{7}$$

where t_f is the integral final time, $Q = Q^T > 0$ is a positive definite weighting matrix that is chosen during specific calculation process, and γ is the attenuation level.

Assumption 3: The desired trajectory signal $x_d(t)$ and its derivative of time $\dot{x}_d(t)$ are supposed to be known and bounded.

Theorem 1: For all $t > 0$, $h_i(\xi(t)) h_j(\xi(t)) \neq 0$ with A_i, $\bar{B}_i$ defined by Eq. (6). If there exists $N_1 = N_1^T > 0$, Y_i, a positive constant α_1 and the attenuation level γ, the next LMI conditions are hold:

$$\begin{bmatrix} T & \bar{I} & H & N_1 E_a^T & N_1 \\ (*) & -\gamma^2 I & 0 & 0 & 0 \\ (*) & (*) & -\alpha_1^{-1} I & 0 & 0 \\ (*) & (*) & (*) & -\alpha_1 I & 0 \\ (*) & (*) & (*) & (*) & -Q^{-1} \end{bmatrix} \leq 0$$

where $T = A_i N_1 + N_1 A_i^T + \bar{B}_i Y_i + Y_i^T \bar{B}_i^T$, that means the dynamic error system (6) is asymptotically stable and the $H\infty$ tracking performance (7) is ensured under the attenuation level γ. Furthermore, if the conditions of LMIs can be solved, the gain K_{h_i} can be calculated by $K_{h_i} = Y_i N_1^{-1}$.

Proof. We consider the Lyapunov function candidate as: $V_1(t) = e(t)^T P_1 e(t)\, with P_1 = P_1^T > 0$. The corresponding time derivative of $V_1(t)$ is obtained as:

$$\begin{aligned} \dot{V}_1(t) &= \sum\nolimits_{i=1,j=1}^{r} h_i(\xi(t)) h_j(\xi(t)) \left[2e(t)^T P_1 \dot{e}(t)\right] \\ &= \sum\nolimits_{i=1,j=1}^{r} h_i(\xi(t)) h_j(\xi(t)) \left[2e(t)^T P_1 \left(A_e e(t) + \bar{I}\vartheta_1\right)\right] \end{aligned} \tag{8}$$

According to Eq. (7), if Eq. (9) satisfies, the stability and tracking issue of the error dynamic model (8) can be ensured under the H_∞ performance with an attenuation level γ:

$$\dot{V}_1(t) + e(t)^T Q e(t) - \gamma^2 \vartheta_1(t)^T \vartheta_1(t) \leq 0 \tag{9}$$

Substituting Eq. (6) into Eq. (9), we obtain the following inequality

$$\begin{aligned} &\sum\nolimits_{i=1,j=1}^{r} h_i(\xi(t)) h_j(\xi(t)) \left[2e(t)^T P_1 \left(A_e e(t) + \bar{I}\vartheta_1\right)\right. \\ &\qquad \left. + e(t)^T Q e(t) - \gamma^2 \vartheta_1(t)^T \vartheta_1(t)\right] \leq 0 \end{aligned} \tag{10}$$

Eq. (10) can be rewritten as:

$$\begin{aligned} &\sum\nolimits_{i=1,j=1}^{r} h_i(\xi(t)) h_j(\xi(t)) \left[e(t)^T \left(P_1 A_e + A_e^T P_1\right) e(t)\right. \\ &\qquad + e(t)^T P_1 \bar{I}\vartheta_1 + \vartheta_1^T \bar{I}^T P_1 e(t) + e(t)^T Q e(t) \\ &\qquad \left. - \gamma^2 \vartheta_1(t)^T \vartheta_1(t)\right] \leq 0 \end{aligned}$$

Obviously, the following inequality is obtained:

$$\begin{bmatrix} e(t) \\ \vartheta_1(t) \end{bmatrix}^T \begin{bmatrix} P_1 A_e + A_e^T P_1 + Q & P_1 \bar{I} \\ (*) & -\gamma^2 I \end{bmatrix} \begin{bmatrix} e(t) \\ \vartheta_1(t) \end{bmatrix} \leq 0 \tag{11}$$

Eq. (11) is equal to:

$$\begin{bmatrix} P_1 A_e + A_e^T P_1 + Q & P_1 \bar{I} \\ (*) & -\gamma^2 I \end{bmatrix} \leq 0 \tag{12}$$

Combing Eq. (6) with Eq. (12), we have:

$$\begin{bmatrix} U & P_1 \bar{I} \\ (*) & -\gamma^2 I \end{bmatrix} \leq 0 \tag{13}$$

then Eq. (13) can be rewritten as: $\Xi + \Delta\Xi \leq 0$ where

$$\begin{aligned} U &= P_1\left(A_i + \Delta A_i + \bar{B}_i K_{h_i}\right) \\ &\quad + \left(A_i + \Delta A_i + \bar{B}_i K_{h_i}\right)^T P_1 + Q \\ \Xi &= \begin{bmatrix} P_1\left(A_i + \bar{B}_i K_{h_i}\right) + \left(A_i + \bar{B}_i K_{h_i}\right)^T P_1 + Q & P_1 \bar{I} \\ (*) & -\gamma^2 I \end{bmatrix} \\ \Delta\Xi &= \begin{bmatrix} P_1 \Delta A_i + \Delta A_i^T P_1 & 0 \\ 0 & 0 \end{bmatrix} \end{aligned}$$

Using Lemma 2 (Schur's complement), the following condition holds:

$$\begin{aligned} P_1 \Delta A_i + \Delta A_i^T P_1 &= P_1 H \Delta a E_a + (H \Delta a E_a)^T P_1 \\ &\leq \alpha_1 P_1 H H^T P_1 + \alpha_1^{-1} E_a^T E_a \end{aligned}$$

Eq. (13) then holds if:

$$\begin{bmatrix} \tilde{U} & P_1 \bar{I} \\ (*) & -\gamma^2 I \end{bmatrix} \leq 0 \tag{14}$$

where $\tilde{U} = P_1 A_i + A_i^T P_1 + P_1 \bar{B}_i K_{h_i} + (\bar{B}_i K_{h_i})^T P_1 + \alpha_1 P_1 H H^T P_1 + \alpha_1^{-1} E_a^T E_a + Q$

By utilizing Schur's complement presented in Lemma 2 and $Y_i = K_{h_i} N_1$ to Eq. (14), the LMI conditions represented in Theorem 1 is satisfied. These results illustrate that the dynamic error system (6) is asymptotically stable and the $H\infty$ tracking performance (7) is ensured under the attenuation level γ. The proof is complete.

B. FAULT DIAGNOSIS

A new state variable $x_s \in R^P$ [44] is introduced to diagnose the SAFs simultaneously that depends on the measured output $y_f(t)$.

$$\dot{x}_s(t) = -A_s x_s(t) + A_s y_f(t) \tag{15}$$

where $-A_s$ is a Hurwitz matrix with compatible dimension.

By combining Eq. (1) with Eq. (15), the augmented system for state and fault estimation can be written as:

$$\begin{cases} \dot{\tilde{x}}_f(t) = \sum\nolimits_{i=1}^{r} h_i(\xi(t))[\tilde{A}_i \tilde{x}_f(t) + \tilde{B}_i u_f(t) \\ \quad + \tilde{F}_i f_a(t) + \tilde{E}_i f_s(t)] \\ \tilde{y}_f(t) = \sum\nolimits_{i=1}^{r} h_i(\xi(t)) \left[\tilde{D}_i \tilde{x}_f(t)\right] \end{cases} \tag{16}$$

where $\tilde{x}_f(t) = \begin{bmatrix} x_f(t) \\ x_s(t) \end{bmatrix}$, $\tilde{A}_i = \begin{bmatrix} \bar{A}_i & 0 \\ A_s C_i & -A_s \end{bmatrix}$,

$$\tilde{B}_i = \begin{bmatrix} \bar{B}_i \\ 0 \end{bmatrix}, \tilde{F}_i = \begin{bmatrix} \bar{F}_i \\ 0 \end{bmatrix}, \tilde{E}_i = \begin{bmatrix} 0 \\ A_s E_i \end{bmatrix}, \tilde{D}_i = \begin{bmatrix} 0 \\ I_p \end{bmatrix}$$

Based on the Eq. (16), in order to estimate the unmeasurable states and SAFs at the same time, we construct the following fuzzy fault diagnosis observer:

$$\begin{aligned}\dot{\hat{\tilde{x}}}_f(t)(t) &= \sum_{i=1}^{r} h_i(\xi(t))[\tilde{A}_i\hat{\tilde{x}}_f(t) + \tilde{B}_i u_f(t) \\ &\quad + \tilde{F}_i\hat{f}_a(t) + \tilde{E}_i\hat{f}_s(t) + L_i\varepsilon(t)] \\ \varepsilon(t) &= \tilde{D}_i(\tilde{x}_f(t) - \hat{\tilde{x}}_f(t)) \\ \dot{\hat{f}}_a(t) &= \sum_{i=1}^{r} h_i(\xi(t))[-\hat{f}_a(t) - L_{f_a}(y_f(t) - \hat{y}_f(t))] \\ \dot{\hat{f}}_s(t) &= \sum_{i=1}^{r} h_i(\xi(t))[-\hat{f}_s(t) - L_{f_s}\varepsilon(t)] \end{aligned} \tag{17}$$

where $\hat{\tilde{x}}_f(t)$ is the estimate state, $\varepsilon(t)$ is the estimate weight vector, $\hat{f}_a(t)$ and $\hat{f}_s(t)$ represent the estimation of SAFs. L_i, L_{f_a}, L_{f_s} are the gain matrices with compatible dimension, which need to be calculated later.

Now, we define: $\tilde{e}_x(t) = \tilde{x}_f(t) - \hat{\tilde{x}}_f(t)$ is the state estimation error, $e_{f_a}(t) = f_a(t) - \hat{f}_a(t)$ and $e_{f_s}(t) = f_s(t) - \hat{f}_s(t)$ are faults error, respectively, $\chi(t) = [\tilde{e}_x^T e_{f_a}^T e_{f_s}^T]^T$ is a comprehensive error matrix for calculation. Combing with Eq. (16), the augmented error system of observation is given as follows:

$$\begin{aligned}\dot{\tilde{e}}_x(t) &= \dot{\tilde{x}}_f(t) - \dot{\hat{\tilde{x}}}_f(t) \\ &= \sum_{i=1,j=1}^{r} h_i(\xi(t))h_j(\xi(t))[\left(\tilde{A}_i - L_i\tilde{D}_i\right)\tilde{e}_x(t) \\ &\quad + \tilde{F}_i e_{f_a}(t) + \tilde{E}_i e_{f_s}(t)]\end{aligned} \tag{18}$$

Similar to Theorem 1, we consider the H_∞ performance of the observation error augmented system. The attenuation of the tracking error for desired trajectory signal can be ensured by using the H_∞ criterion with regard to the disturbance error $\chi(t)$ as follow:

$$\int_0^{t_f}\chi(t)^T\tilde{Q}\chi(t)\,dt \le \gamma^2\int_0^{t_f}\Theta_1(t)^T\Theta_1(t)dt \tag{19}$$

where t_f denotes the final time, $\tilde{Q} = \tilde{Q}^T = diag[Q_1, Q_2, Q_3] > 0$ is a positive definite weighting matrix that is chosen during specific calculation process, and γ is the attenuation level.

Theorem 2: For all $t > 0$, $h_i(\xi(t))h_j(\xi(t)) \neq 0$ with $\tilde{\tilde{A}}_i$, $\tilde{C}_i$, $\tilde{D}_i$, $\tilde{E}_i$, E_i defined by Eq. (18). If there exists $P_2 = P_2^T > 0$, $R_1 > 0$, $R_2 > 0$, Z_1, Z_2, Z_3, a positive constant α_1 and the attenuation level γ, the next LMI conditions are hold as shown at the bottom of the page, where $W = P_2\tilde{\tilde{A}}_i + \tilde{\tilde{A}}_i^T P_2 - Z_1\tilde{D}_i - \tilde{D}_i^T Z_1 + Q_1$, that means the dynamic error system (18) is asymptotically stable and the $H\infty$ tracking performance (19) is ensured under the attenuation level γ. Furthermore, if the conditions of LMIs can be solved, the gains L_i, L_{f_a}, L_{f_s} can be obtained by using $L_i = P_2^{-1}Z_1$, $L_{f_a} = R_1^{-1}Z_2$, $L_{f_s} = R_2^{-1}Z_3$.

*Proof.*The next candidate Lyapunov function is chosen: $V_2 = \tilde{e}_x^T(t)P_2\tilde{e}_x(t) + e_{f_a}^T(t)R_1 e_{f_a}(t) + e_{f_s}^T(t)R_2 e_{f_s}(t)$ with $P_2 = P_2^T > 0$, $R_1 > 0$, $R_2 > 0$.

According to Eq. (19), if the following inequality satisfies, the stability of the dynamic error system can be ensured under the H_∞ performance with an specific attenuation level γ:

$$\dot{V}_2(t) + \chi(t)^T\tilde{Q}\chi(t) - \gamma^2\Theta_1(t)^T\Theta_1(t) \le 0 \tag{20}$$

Eq. (20) can be rewritten as:

$$\begin{aligned}\sum_{i=1,j=1}^{r} & h_i(\xi(t))h_j(\xi(t))[2\tilde{e}_x^T(t)P_2\dot{\tilde{e}}_x(t) \\ &+ 2e_{f_a}^T(t)R_1\dot{e}_{f_a}(t) + 2e_{f_s}^T(t)R_2\dot{e}_{f_s}(t) \\ &+ \chi(t)^T\tilde{Q}\chi(t) - \gamma^2\Theta_1(t)^T\Theta_1(t)] \le 0\end{aligned} \tag{21}$$

Substituting (18) into (21), we obtain the following inequality:

$$\begin{aligned}\sum_{i=1,j=1}^{r} & h_i(\xi(t))h_j(\xi(t))[2\tilde{e}_x^T(t)P_2((\tilde{A}_i \\ &- L_i\tilde{D}_i)\tilde{e}_x(t) + \tilde{F}_i e_{f_a}(t) + \tilde{E}_i e_{f_s}(t)) \\ &+ 2e_{f_a}^T(t)R_1\left(\dot{f}_a(t) - \dot{\hat{f}}_a(t)\right) \\ &+ 2e_{f_s}^T(t)R_2(\dot{f}_s(t) - \dot{\hat{f}}_s(t))] + \chi(t)^T\tilde{Q}\chi(t) \\ &- \gamma^2\Theta_1(t)^T\Theta_1(t) \le 0\end{aligned}$$

Using Eq. (17), the next inequality can be given as:

$$\begin{aligned}\sum_{i=1,j=1}^{r} & h_i(\xi(t))h_j(\xi(t))[2\tilde{e}_x^T(t)P_2((\tilde{A}_i \\ &- L_i\tilde{D}_i)\tilde{e}_x(t) + \tilde{F}_i e_{f_a}(t) + \tilde{E}_i e_{f_s}(t)) \\ &+ 2e_{f_a}^T(t)R_1(\dot{f}_s(t) + \hat{f}_a(t) + L_{f_a}\tilde{C}_i(\tilde{e}_x(t) \\ &+ E_i e_{f_s}(t))) + 2e_{f_s}^T(t)R_2(\dot{f}_s(t) + \hat{f}_s(t) + L_{f_s}\tilde{D}_i\tilde{e}_x(t))] \\ &+ \chi(t)^T\tilde{Q}\chi(t) - \gamma^2\Theta_1(t)^T\Theta_1(t) \le 0\end{aligned} \tag{22}$$

$$\begin{bmatrix} W & P_2\tilde{F}_i + \left(Z_2\tilde{C}_i\right)^T & P_2\tilde{E}_i + \left(Z_3\tilde{D}_i\right)^T & 0 & 0 & P_2\tilde{H} & \tilde{E}_a^T \\ (*) & -2R_1 + Q_2 & Z_2E_i & R_1 & 0 & 0 & 0 \\ (*) & (*) & -2R_2 + Q_3 & 0 & R_2 & 0 & 0 \\ (*) & (*) & (*) & -\gamma^2 I & 0 & 0 & 0 \\ (*) & (*) & (*) & (*) & -\gamma^2 I & 0 & 0 \\ (*) & (*) & (*) & (*) & (*) & -\alpha_2^{-1}I & 0 \\ (*) & (*) & (*) & (*) & (*) & (*) & -\alpha_2 I \end{bmatrix} \le 0$$

Eq. (22), it can be rewritten as:

$$\begin{aligned}&\sum\nolimits_{i=1,j=1}^{r} h_i(\xi(t))\, h_j(\xi(t))\, [2\tilde{e}_x^T(t) P_2(\tilde{A}_i\\&- L_i\tilde{D}_i)\tilde{e}_x(t) + 2\tilde{e}_x^T(t) P_2\tilde{F}_i e_{f_a}(t) + \tilde{e}_x^T(t) P_2\tilde{E}_i e_{f_s}(t)\\&+ 2e_{f_a}^T(t) R_1\left(\dot{f}_a(t) + f_a(t)\right) - 2e_{f_a}^T(t) R_1 e_{f_a}\\&+ 2e_{f_a}^T(t) R_1 L_{f_a}\tilde{C}_i\tilde{e}_x(t) + 2e_{f_a}^T(t) R_1 L_{f_a} E_i e_{f_s}(t)\\&+ 2e_{f_s}^T(t) R_2(\dot{f}_s(t) + f_s(t)) - 2e_{f_s}^T(t) R_2 e_{f_s}(t)\\&+ 2e_{f_s}^T(t) R_2 L_{f_s}\tilde{D}_i\tilde{e}_x(t)] + \chi(t)^T\tilde{Q}\chi(t)\\&- \gamma^2\Theta_1(t)^T\Theta_1(t) \le 0\end{aligned}$$

It can be further expressed as:

$$\begin{aligned}&\sum\nolimits_{i=1,j=1}^{r} h_i(\xi(t))\, h_j(\xi(t))\, [\chi^T(t)(\Omega_1 + \tilde{Q})\chi(t)\\&+ 2\chi^T(t)\Theta_1 - \gamma^2\Theta_1(t)^T\Theta_1(t)] \le 0\end{aligned}$$

where as (23), shown at the bottom of the page. Then Eq. (23) can be rewritten as:

$$\Gamma + \Delta\Gamma \le 0 \tag{24}$$

where as shown at the bottom of the next page. Using Lemma 2 (Schur's complement), we obtain the following inequality:

$$\begin{aligned}P_2\Delta\tilde{A}_i + \Delta\tilde{A}_i^T P_2 &= P_2\tilde{H}\Delta a\tilde{E}_a + \left(\tilde{H}\Delta a\tilde{E}_a\right)^T P_2\\&\le \alpha_2 P_2\tilde{H}\tilde{H}^T P_2 + \alpha_2^{-1}\tilde{E}_a^T\tilde{E}_a\end{aligned} \tag{25}$$

Using Eq. (25), Eq. (24) then holds if as (26), shown at the bottom of the next page, where $\hat{W} = P_2\left(\tilde{\tilde{A}}_i - L_i\tilde{D}_i\right) + \left(\tilde{\tilde{A}}_i - L_i\tilde{D}_i\right)^T P_2$

$$+\alpha_2 P_2\tilde{H}\tilde{H}^T P_2 + \alpha_2^{-1}\tilde{E}_a^T\tilde{E}_a + Q_1$$

By utilizing Schur's complement presented in Lemma 2 and $Z_1 = P_2 L_i, Z_2 = R_1 L_{f_a}, Z_3 = R_2 L_{f_s}$ to Eq. (26), the LMI conditions represented in Theorem 2 is satisfied. These results illustrate that the dynamic error system (18) is asymptotically stable and the $H\infty$ tracking performance (19) is ensured under the attenuation level γ. The proof is complete.

C. FTTC DESIGN

Up to present, the estimation of system states and SAFs have been obtained by solving the LMIs proposed in Theorem 2. The following important issue is to design an effective control law to compensate the sensor and actuator fault so that the states of the system can track desired trajectory precisely after the sensor fault and actuator fault occur simultaneously.

We define $e_x(t) = x(t) - x_f(t)$, $e_y(t) = y(t) - y_f(t)$ as the error of the state with fault and without fault. Then, we define a new state variable as: $z(t) = \begin{bmatrix} e_x(t) \\ \int_0^t e_y(t)\, dt\end{bmatrix}$, and $e_z(t) = z(t) - \hat{z}(t)$ represent the error of $z(t)$ and its estimation. The augmented system can be easily obtained as follows:

$$\begin{aligned}\dot{z}(t) = &\sum\nolimits_{i=1}^{r} h_i(\xi(t))\, [\breve{A}_i z(t) + \breve{B}_i\left(u(t) - u_f(t)\right)\\&+ \breve{F}_i f_a(t) + \breve{E}_i f_s(t)]\end{aligned} \tag{27}$$

where $\breve{A}_i = \begin{bmatrix}\bar{A}_i & 0\\ C_i & 0\end{bmatrix}, \breve{B}_i = \begin{bmatrix}\bar{B}_i\\ 0\end{bmatrix}, \breve{F}_i = \begin{bmatrix}-\bar{F}_i\\ 0\end{bmatrix}, \breve{E} = \begin{bmatrix}0\\ -E_i\end{bmatrix}$

Now, we define a new fault tolerant control law:

$$\begin{aligned}u(t) - u_f(t) = &K_{P_i}\left(x(t) - \hat{x}_f(t)\right)\\&+ K_{I_i}\int_0^t \left(y(t) - y_f(t)\right) dt - \hat{f}_a(t)\\&- \hat{f}_s(t)\end{aligned} \tag{28}$$

where $K_{PI_i} = [K_{P_i}, K_{I_i}]$.

Then, substituting Eq. (28) into Eq. (27), the augmented system can be expressed as:

$$\begin{aligned}\dot{z}(t) = &\sum\nolimits_{i=1}^{r} h_i(\xi(t))\, [\left(\breve{A}_i + \breve{B}_i K_{PI_i}\right) z(t)\\&- \breve{B}_i K_{PI_i} e_z + \breve{B}_i e_{f_a} + \breve{B}_i e_{f_s} + \left(\breve{F}_i - \breve{B}_i\right) f_a(t)\\&+ (\breve{E}_i - \breve{B}_i) f_s(t)]\end{aligned} \tag{29}$$

Theorem 3: For all $t > 0$, $h_i(\xi(t))\, h_j(\xi(t)) \neq 0$ with $\breve{\tilde{A}}_i$, $\breve{B}_i$ defined by Eq. (29). If there exists $P_3 = P_3^T > 0$, $P_4 =$

$$\begin{aligned}&\Omega_1 + \tilde{Q} = \begin{bmatrix}\tilde{W} & P_2\tilde{F}_i + \left(R_1 L_{f_a}\tilde{C}_i\right)^T & P_2\tilde{E}_i + \left(R_2 L_{f_s}\tilde{D}_i\right)^T & 0 & 0\\ (*) & -2R_1 + Q_2 & R_1 L_{f_a} E_i & R_1 & 0\\ (*) & (*) & -2R_2 + Q_3 & 0 & R_2\\ (*) & (*) & (*) & -\gamma^2 I & 0\\ (*) & (*) & (*) & (*) & -\gamma^2 I\end{bmatrix} \le 0\\&\tilde{A}_i = \tilde{\tilde{A}}_i + \Delta\tilde{A}_i,\ \Delta\tilde{A}_i = \begin{bmatrix}\Delta A_i & 0\\ 0 & 0\end{bmatrix},\\&\tilde{\tilde{A}}_i = \begin{bmatrix}A_i & 0\\ A_s D_i & -A_s\end{bmatrix},\ \Theta_1 = \begin{bmatrix}0\\ R_1(\dot{f}_a(t) + f_a(t))\\ R_2(\dot{f}_s(t) + f_s(t))\end{bmatrix}\\&\tilde{W} = P_2\left(\tilde{A}_i - L_i\tilde{D}_i\right) + \left(\tilde{A}_i - L_i\tilde{D}_i\right)^T P_2 + Q_1\end{aligned} \tag{23}$$

$P_4^T > 0$, and a positive constant α_3, α_4, β_1, β_2 and β_3, such that the next LMI conditions are held: $\begin{bmatrix} \Gamma & \Pi \\ (*) & \Psi \end{bmatrix} \leq 0$ where

Γ

$$= \begin{bmatrix} P_3\check{\breve{A}}_i + \check{\breve{A}}_i^T P_3 & 0 & P_3 & \left(\breve{B}_i K_{PI_i}\right)^T \\ (*) & P_4\check{\breve{A}}_i + \check{\breve{A}}_i^T P_4 & 0 & 0 \\ (*) & (*) & -(\beta_2+\beta_1)^{-1} I & 0 \\ (*) & (*) & (*) & -\beta_2 I \end{bmatrix}$$

Π

$$= \begin{bmatrix} P_3\breve{H} & \breve{E}_a^T & 0 & 0 & 0 & 0 \\ 0 & 0 & P_4 & \left(\breve{B}_i K_{PI_i}\right)^T & P_4\breve{H} & \breve{E}_a^T \\ 0 & 0 & 0 & 0 & 0 & 0 \\ 0 & 0 & 0 & 0 & 0 & 0 \end{bmatrix}$$

Ψ

$$= \begin{bmatrix} -\alpha_3^{-1} I & 0 & 0 & 0 & 0 & 0 \\ (*) & -\alpha_3 I & 0 & 0 & 0 & 0 \\ (*) & (*) & -\beta_3^{-1} I & 0 & 0 & 0 \\ (*) & (*) & (*) & -(\beta_3^{-1}+\beta_1^{-1})^{-1} & 0 & 0 \\ (*) & (*) & (*) & (*) & -\alpha_4^{-1} I & 0 \\ (*) & (*) & (*) & (*) & (*) & -\alpha_4 I \end{bmatrix}$$

that means the dynamic error system (29) is asymptotically stable. Furthermore, if the conditions of LMIs can be solved, the gains K_{PI_i} can be obtained.

Proof. The following Lyapunov function is chosen as: $V_3(t) = z^T(t) P_3 z(t) + e_z^T(t) P_4 e_z(t)$ with $P_3 = P_3^T > 0$, $P_4 = P_4^T > 0$

The time-derivative of $V_3(t)$ is formulated as:

$$\dot{V}_3(t) = \sum\nolimits_{i=1,j=1}^{r} h_i(\xi(t)) h_j(\xi(t)) \times \left[2z^T(t) P_3 \dot{z}(t) + 2e_z^T(t) P_4 \dot{e}_z(t)\right] \quad (30)$$

Substituting Eq. (29) into Eq. (30) and Using Lemma 1, we have:

$$\begin{aligned} \dot{V}_3(t) \leq & \sum\nolimits_{i=1,j=1}^{r} h_i(\xi(t)) h_j(\xi(t)) [z^T(t)(P_3\left(\check{A}_i + \breve{B}_i K_{PI_i}\right) \\ & + \left(\check{A}_i + \breve{B}_i K_{PI_i}\right)^T P_3) z(t) \\ & + e_z^T(t)\left(P_4\left(\check{A}_i + \breve{B}_i K_{PI_i}\right) + \left(\check{A}_i + \breve{B}_i K_{PI_i}\right)^T P_4\right) \\ & \times e_z(t) - 2z^T(t) P_3 \breve{B}_i K_{PI_i} e_z + 2z^T(t) P_3 \breve{B}_i e_{f_a} \\ & + 2z^T(t) P_3 \breve{B}_i e_{f_s} \\ & + 2z^T(t) P_3\left(\breve{F}_i - \breve{B}_i\right) f_a(t) \\ & + 2z^T(t) P_3\left(\breve{E}_i - \breve{B}_i\right) f_s(t)] \\ \leq & \sum\nolimits_{i=1,j=1}^{r} h_i(\xi(t)) h_j(\xi(t)) \\ & \times \left[\varsigma^T(t)\Omega_2(t)\varsigma(t) + \varsigma^T(t)\Theta_2\right] \\ \leq & \sum\nolimits_{i=1,j=1}^{r} h_i(\xi(t)) h_j(\xi(t)) \\ & [-\lambda_{min}(\Omega_2(t))\|\varsigma(t)\|^2 + \|\Theta_2\|\varsigma(t)] \\ \leq & \sum\nolimits_{i=1,j=1}^{r} h_i(\xi(t)) h_j(\xi(t)) \\ & \times [-\tau_1(\|\varsigma(t)\| - \frac{\tau_2}{\tau_1})^2 + \frac{\tau_2^2}{\tau_1}] \end{aligned}$$

where $\lambda_{min}(\Omega_2(t))$ denotes the smallest eigenvalue of $\Omega_2(t)$, and $\tau_1 = -\lambda_{min}(\Omega_2(t))$, $\varsigma(t) = [z(t) e_z(t)]^T$

Θ_2

$$\Gamma = \begin{bmatrix} \tilde{W} & P_2\tilde{F}_i + \left(R_1 L_{f_a}\tilde{C}_i\right)^T & P_2\tilde{E}_i + \left(R_2 L_{f_s}\tilde{D}_i\right)^T & 0 & 0 \\ (*) & -2R_1 + Q_2 & R_1 L_{f_a} E_i & R_1 & 0 \\ (*) & (*) & -2R_2 + Q_3 & 0 & R_2 \\ (*) & (*) & (*) & -\gamma^2 I & 0 \\ (*) & (*) & (*) & (*) & -\gamma^2 I \end{bmatrix}$$

$$\Delta\Gamma = \begin{bmatrix} P_2\Delta\tilde{A}_i + \Delta\tilde{A}_i^T P_2 & 0 & 0 & 0 & 0 \\ 0 & 0 & 0 & 0 & 0 \\ 0 & 0 & 0 & 0 & 0 \\ 0 & 0 & 0 & 0 & 0 \\ 0 & 0 & 0 & 0 & 0 \end{bmatrix}$$

$$\begin{bmatrix} \hat{W} & P_2\tilde{F}_i + \left(R_1 L_{f_a}\tilde{C}_i\right)^T & P_2\tilde{E}_i + \left(R_2 L_{f_s}\tilde{D}_i\right)^T & 0 & 0 \\ (*) & -2R_1 + Q_2 & R_1 L_{f_a} E_i & R_1 & 0 \\ (*) & (*) & -2R_2 + Q_3 & 0 & R_2 \\ (*) & (*) & (*) & -\gamma^2 I & 0 \\ (*) & (*) & (*) & (*) & -\gamma^2 I \end{bmatrix} \leq 0 \quad (26)$$

$$= \begin{bmatrix} 2P_3(\breve{B}_i e_{f_a} + \breve{B}_i e_{f_s} + \left(\breve{F}_i - \breve{B}_i\right) f_a(t) + \left(\breve{E}_i - \breve{B}_i\right) f_s(t)) \\ 0 \end{bmatrix} \tag{31}$$

Now, we aim to obtain the gain K_{PI_i} such that stability of the augmented system (29) can be guaranteed. Therefore, the Eq. (31) should be satisfied:

$$\Omega_2(t) = \begin{bmatrix} G & -P_3\breve{B}_i K_{PI_i} \\ (*) & J \end{bmatrix} \leq 0 \tag{32}$$

where $G = P_3\left(\breve{A}_i + \breve{B}_i K_{PI_i}\right) + \left(\breve{A}_i + \breve{B}_i K_{PI_i}\right)^T P_3$,
$J = P_4\left(\breve{A}_i + \breve{B}_i K_{PI_i}\right) + \left(\breve{A}_i + \breve{B}_i K_{PI_i}\right)^T P_4$

Then, Eq. (32) can be given as:
$\begin{bmatrix} \tilde{G} & -P_3\breve{B}_i K_{PI_i} \\ (*) & \tilde{J} \end{bmatrix} \leq 0$ Where $\breve{A}_i = \breve{\bar{A}}_i + \Delta\breve{A}_i$, $\breve{\bar{A}}_i = \begin{bmatrix} A_i & 0 \\ C_i & 0 \end{bmatrix}$, $\Delta\breve{A}_i = \begin{bmatrix} \Delta A_i & 0 \\ 0 & 0 \end{bmatrix}$ $\tilde{G} = P_3\left(\breve{\bar{A}}_i + \breve{B}_i K_{PI_i}\right) + \left(\breve{\bar{A}}_i + \breve{B}_i K_{PI_i}\right)^T P_3 + P_3\Delta\breve{A}_i + \Delta\breve{A}_i^T P_3$
$\tilde{J} = P_4\left(\breve{\bar{A}}_i + \breve{B}_i K_{PI_i}\right) + \left(\breve{\bar{A}}_i + \breve{B}_i K_{PI_i}\right)^T P_4 + P_4\Delta\breve{A}_i + \Delta\breve{A}_i^T P_4$ Using Lemma 1, we have:

$$\begin{bmatrix} \Lambda_{11} & 0 \\ 0 & \Lambda_{22} \end{bmatrix} \leq 0 \tag{33}$$

where

$$\begin{aligned} \Lambda_{11} &= P_3\breve{\bar{A}}_i + \breve{\bar{A}}_i^T P_3 + (\beta_2 + \beta_1) P_3 P_3 \\ &\quad + \beta_2^{-1}\left(\breve{B}_i K_{PI_i}\right)^T \breve{B}_i K_{PI_i} + \alpha_3 P_3 H H^T P_3 \\ &\quad + \alpha_3^{-1} E_a^T E_a \\ \Lambda_{22} &= P_4\breve{\bar{A}}_i + \breve{\bar{A}}_i^T P_4 + \beta_3 P_4 P_4 + (\beta_3^{-1} \\ &\quad + \beta_1^{-1})\left(\breve{B}_i K_{PI_i}\right)^T \breve{B}_i K_{PI_i} + \alpha_4 P_4 H H^T P_4 \\ &\quad + \alpha_4^{-1} E_a^T E_a \end{aligned}$$

By utilizing Schur's complement presented in Lemma 2 to Eq. (33), the LMI conditions represented in Theorem 3 is satisfied. These results illustrate that the dynamic error system (29) is asymptotically stable. Furthermore, if the conditions of LMIs can be solved, the gains K_{PI_i} can be obtained. The proof is complete.

Remark 2: The block scheme of FTTC is shown in FIGURE 1. The FTTC is designed to estimate and compensate the SAFs simultaneously which ensures the achievement of a good tracking performance. Whereas, researches in many articles are only investigated a single fault (sensor fault or actuator fault).

Remark 3: All the states of the nonlinear system are unmeasurable, the states of the reference model can be calculated. The output of the faulty system is measurable. Utilizing the proposed method, all the states of the system can be estimated by using the value of the output of the faulty system.

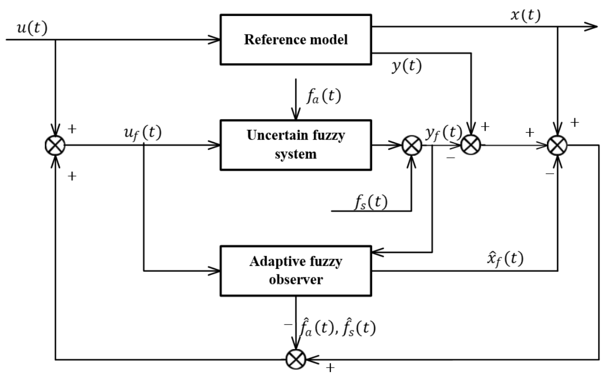

FIGURE 1. The block scheme of FTTC.

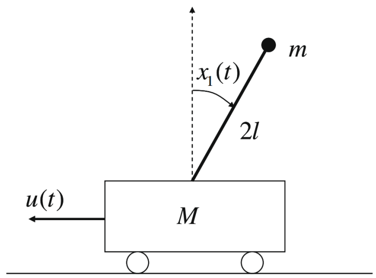

FIGURE 2. Inverted pendulum on a cart.

IV. EXAMPLE AND SIMULATION

The validity of the mentioned observer-based faults tolerant tracking controller is illustrated in this section by two practical examples: Inverted Pendulum on a Cart (Figure 2) and Overhead Crane System (Figure 12). Firstly, three different types of actuator faults have been applied in a inverted pendulum on a cart system to show the performance of the compensation and tracking of our method. For further explanation, an contrast work with the method investigated in [45] have been carried out to illustrate the advantage of our approach. Finally, an overhead crane system (Figure 3) using our method is utilized to give the compared result with non-FTC method.

Example 1 (Inverted Pendulum on a Cart): The angular position tracking issue of an inverted pendulum system with SAFs and uncertainty is considered to illustrate our proposed FTTC approach. The dynamic system is represented as:

$$\begin{cases} \dot{x}_{f_1} = x_{f_2} \\ \dot{x}_{f_2} = \dfrac{(m+M)g\sin(x_{f_1}) - mlx_{f_2}^2\sin(x_{f_1})\cos(x_{f_1}) - \cos(x_{f_1})u}{l(\frac{1}{3}m + \frac{4}{3}M + m\sin^2(x_{f_1}))} + f_a \\ y_f = \begin{bmatrix} 1 & 0 \\ 0 & 1 \end{bmatrix}\begin{bmatrix} x_{f_1} \\ x_{f_2} \end{bmatrix} + \begin{bmatrix} 0 \\ 1 \end{bmatrix} f_s \end{cases} \tag{34}$$

where x_1 and x_2 represent the angular position and velocity of the inverted pendulum system, respectively. $u(t)$ is control input to the cart.

In this example, in order to meet real-world engineering conditions, we choose the same parameters as [46]: $m = 0.1kg$ and $M = 1kg$ represent the masses of the inverted pendulum and cart, respectively, $2l = 1m$ is the length of the pendulum, $g = 9.8m/s^2$. In order to simplify the design process, the angular position is assumed to be chosen as: $-\pi/6 \leq x_{f_1} \leq \pi/6$, and the angle velocity is selected as: $-0.5 \leq x_{f_1} \leq 0.5$. Note that $m\sin^2(x_{f_1})$ is small regarding to $\frac{1}{3}m + \frac{4}{3}M$, it is assumed to be neglected. Moreover, angle x_{f_1} is small such that $\lim_{t-0} \frac{\sin(x_{f_1})}{x_{f_1}} = 0$ is satisfied. Therefore, Eq. (34) can be expressed as follows:

$$\begin{bmatrix} \dot{x}_{f_1} \\ \dot{x}_{f_2} \end{bmatrix} = \begin{bmatrix} 0 & 1 \\ \frac{(m+M)g - mlx_{f_2}^2 \cos(x_{f_1})}{l\left(\frac{1}{3}m + \frac{4}{3}M\right)} & 0 \end{bmatrix} \begin{bmatrix} x_1 \\ x_2 \end{bmatrix} + \begin{bmatrix} 0 \\ \frac{-\cos(x_{f_1})}{l(\frac{1}{3}m+\frac{4}{3}M)} \end{bmatrix} u + \begin{bmatrix} 0 \\ 1 \end{bmatrix} f_a$$

$$y_f = \begin{bmatrix} 1 & 0 \\ 0 & 1 \end{bmatrix} \begin{bmatrix} x_{f_1} \\ x_{f_2} \end{bmatrix} + \begin{bmatrix} 0 \\ 1 \end{bmatrix} f_s$$

Considering the premise variables as $\xi_1 = x_{f_2}^2 \cos\left(x_{f_1}\right)$ and $\xi_2 = \cos\left(x_{f_1}\right)$, for the region : $-\pi/6 \leq x_{f_1} \leq \pi/6$ and $-0.5 \leq x_{f_2} \leq 0.5$, we have:

$\xi_1 = M_1 a_1 + M_2 a_2$, $\xi_2 = N_1 b_1 + N_2 b_2$, $M_1 = \frac{a_1 - \xi_1}{a_1 - a_2}$, $M_2 = 1 - M_1$, $a_1 = max\xi_1 = 0.25$, $a_2 = min\xi_1 = 0$,

$N_1 = \frac{b_1 - \xi_1}{b_1 - b_2}$, $N_2 = 1 - N_1$, $b_1 = max\xi_2 = 1$, $a_2 = min\xi_2 = \sqrt{3}/2$.

Thus, the inverted pendulum system (34) is expressed as the next T-S fuzzy model:

Rule *i*: if $\xi_1(t)$ is $M_{1i}$and$\xi_2(t)$ isN_{2i}

then $\begin{cases} \dot{x}_f(t) = \bar{A}_i x_f(t) + \bar{B}_i u_f(t) + \bar{F}_i f_a(t) \\ y_f(t) = C_i x_f(t) + E_i f_s(t) \end{cases}$ for $i = 1, 2, 3, 4$ where $\bar{A}_i = \begin{bmatrix} 0 & 1 \\ \frac{(m+M)g - ml\xi_1}{l(\frac{1}{3}m+\frac{4}{3}M)} & 0 \end{bmatrix}$, $\bar{B}_i = \begin{bmatrix} 0 \\ \frac{-\xi_2}{l(\frac{1}{3}m+\frac{4}{3}M)} \end{bmatrix}$,

$\bar{F}_i = E_i = \begin{bmatrix} 0 \\ 1 \end{bmatrix}$, $C_i = \begin{bmatrix} 1 & 0 \\ 0 & 1 \end{bmatrix}$.

Uncertain matrix is chosen as: $H = \begin{bmatrix} 0 \\ 2 \end{bmatrix}$, $E_a = [10]$, $\tilde{H} = \check{H} = [0\ 2\ 0\ 0]^T$, $\tilde{E}_a = \check{E}_a = [1\ 0\ 0\ 0]$.

In the fault free case, parameters in Theorem 1 are chosen as: $Q = 10^{-3} \times I_{2\times 2}$, $\alpha_1 = 0.1$. We can obtain the feedback gains K_{h_i} for $i = 1, 2, 3, 4$ by solving the LMI conditions represented in Theorem 1.

$$K_{h_1} = [431.4511\ 99.0019]$$
$$K_{h_2} = [382.2937\ 82.7523]$$
$$K_{h_3} = [550.9974\ 123.8027]$$
$$K_{h_4} = [339.5736\ 74.3023]$$

In the post-fault case, for the purpose of the design of the fuzzy faults and states observer according to Theorem 2, corresponding parameters is first selected as: $Q_1 = 10^{-3} \times I_{4\times 4}$, $Q_2 = Q_3 = 10^{-3}$, $\alpha_2 = 1$. In the sequel, by solving the LMI conditions in Theorem 2, the observer gains L_i, L_{fa_i}, L_{fs_i} for $i = 1, 2, 3, 4$ are calculated.

$$L_1 = L_2 = 10^3 \times \begin{bmatrix} -0.1132\ 0.8039 \\ -0.5006\ 3.2391 \\ -0.0115\ 0.0799 \\ -0.0053\ 0.0174 \end{bmatrix},$$
$$L_{fa_1} = L_{fa_2} = 10^9 \times [2.6678 - 0.7118],$$
$$L_{fs_1} = L_{fs_2} = 10^{11} \times [0.4286 - 1.6296]$$
$$L_3 = L_4 = 10^3 \times \begin{bmatrix} -0.1615\ 1.0986 \\ -0.6998\ 4.4673 \\ -0.0170\ 0.1138 \\ -0.0063\ 0.0223 \end{bmatrix},$$
$$L_{fa_3} = L_{fa_4} = 10^8 \times [8.0108 - 2.1173],$$
$$L_{fs_3} = L_{fs_4} = 10^{10} \times [1.5323 - 6.6513]$$

In Theorem 3, we choose the parameters as: $\alpha_3 = \alpha_4 = 0.1$, $\beta_1 = \beta_2 = \beta_3 = 1$. Then, the control gains K_{PI_i} for $i = 1, 2, 3, 4$ are computed.

$$K_{PI_{i1}} = [159.634893.911615.8814 - 1.1147]$$
$$K_{PI_2} = [144.338490.287313.23630.6195]$$
$$K_{PI_3} = [152.5033113.095513.53690.0187]$$
$$K_{PI_4} = [134.7337110.612712.7018 - 0.1958]$$

The initial system states $x(0) = [0.10]$, $\hat{x}(0) = [0.050]$ and the reference trajectory $x_d(t) = [0.15\sin(1.5t)0.15 \times 1.5\cos(1.5t)]$ are used in this example.

Aiming to evaluate our proposed scheme, two different sensor and actuator faults are chosen in Case 1 and Case 2 to explain the effectiveness of the proposed approach in fault diagnosis and tolerant. And, in Case 3, the control approach in Bouarar et al. [45] is utilized as a comparison to explain the advantage of the mentioned approach.

Case 1. Exponential actuator fault

In this Case, we select the SAFs signal as following:

$$f_s = \begin{cases} 1.5\sin(t-1) & 5 \leq t < 12 \\ 0 & else \end{cases}$$

$$f_a = \begin{cases} 52(1 - 1.5\sin(t-8))\exp(-0.5t)8 \leq t < 20 \\ 0\ \ else \end{cases}$$

According to Theorem 1-3 and observer (17) based control law (28), not only converge the states to the reference trajectories but also estimate the SAFs vectors at the same time.

Figure 3. represents the reference states, faulty system states and their estimates. The control input of reference model and fault tolerant tracking control signal are illustrated in Figure 4. Sensor fault f_s, actuator fault f_a, and its estimate are given in Figure 5. It is noted that the mentioned fuzzy observer is not only able to estimate SAFs accurately, but also estimate the states of the faulty system precisly. Despite the time-varying bounded uncertainties, a desired estimate quality can be obtained.

Furthermore, the simulation process can be divided into three key areas. In the first parts, at $5 \leq t < 8$, only sensor

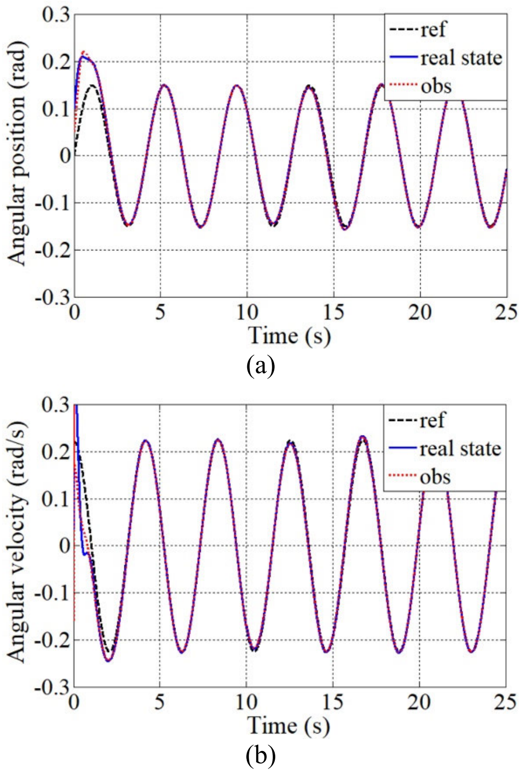

FIGURE 3. Reference states, states of faulty system and their estimates. Black dashed lines show reference signals, blue solid lines represent the real states obtained by the mentioned scheme, red dashed lines give the observed states. (a) angular position. (b) angular velocity.

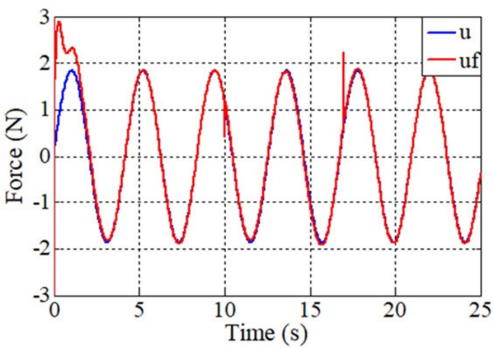

FIGURE 4. Reference and FTTC control signals. blue solid line show the control input signal of nominal system, red solid line show the control input signal with FTTC.

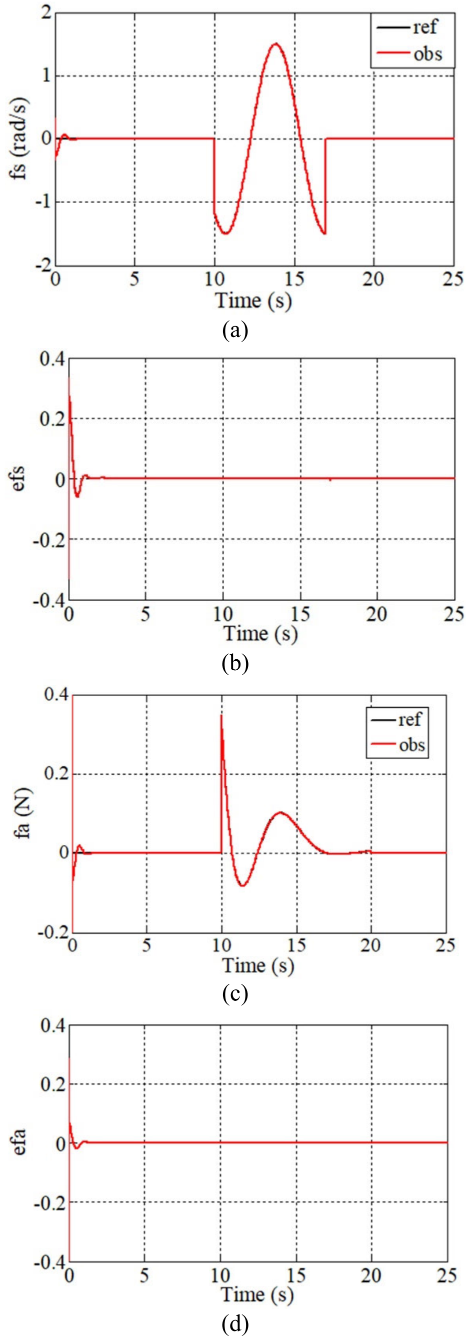

FIGURE 5. Sensor fault $\mathbf{f_s}$, actuator fault $\mathbf{f_a}$, its estimate and the error. Black dashed lines show reference faults signal, red solid lines represent the observed faults. (a) sensor fault $\mathbf{f_s}$ and its estimate. (b) the error of $\mathbf{f_s}$ and its estimate. (c) actuator fault $\mathbf{f_a}$, and its estimate. (d) the error of $\mathbf{f_a}$ and its estimate.

fault is applied in the system. After that, at $8 \le t < 12$, both SAFs apply in the system. At last, at $12 \le t < 20$, the actuator fault is considered. It is obviously observed that, despite in the presence of both sensor and actuator faults, the mentioned fuzzy observer estimates unmeasurable states and faults precisely in Figure 3 and Figure 5, the FTTC law compensates the SAFs simultaneously and ensures the tracking performance of the faulty system. Figure 5(b) and Figure 5(d) shows that the error between the estimated value and the actual value are not exceed 2% at the steady stage of simulation.

Case 2. Time-varying actuator fault

In [39] and [45], only constant actuator fault is considered. In order to show the advantage of our method, the time varying actuator fault signal is considered in this case. The sensor and actuator faults are chosen as:

$$f_s = \begin{cases} 2\sin(t-10)\ 10 \le t < 20 \\ 0, \qquad\qquad\qquad\qquad else \end{cases}$$

$$f_a = \begin{cases} 0.7 + \left(\dfrac{0.05}{5}\right) t\, 14 \le t < 25 \\ 0, \qquad\qquad\qquad\qquad else \end{cases}$$

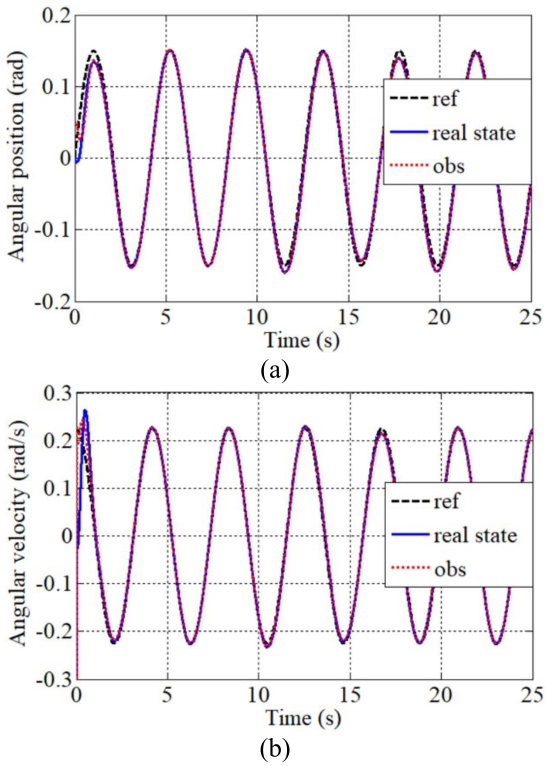

FIGURE 6. Reference states, states of faulty system and their estimates. Black dashed lines show reference signal, blue solid lines represent the real states of the faulty system obtained by the proposed approach, red dashed lines give the observed states. (a) angular position. (b) angular velocity.

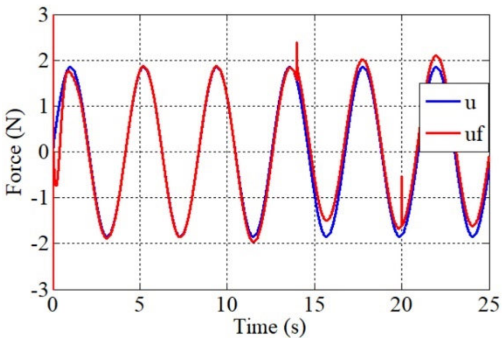

FIGURE 7. Reference and FTC signals. blue solid line show the control input signal of reference model, red solid line show the control input signal with FTC.

The simulation results are given in Figure 6 - Figure 8. Despite the time varying actuator fault signal is applied in the dynamic system, a satisfied estimate quality can be obtained and the FTTC method compensates the sensor and actuator fault effect and ensures the states of the faulty system convergence to the reference signal.

Case 3. Comparison results

The actuator and sensor faults have the following form in this case:

$$f_s = \begin{cases} 2\sin(t-6) \; 10 \le t < 17 \\ 0, \qquad\qquad\qquad\quad else \end{cases}$$

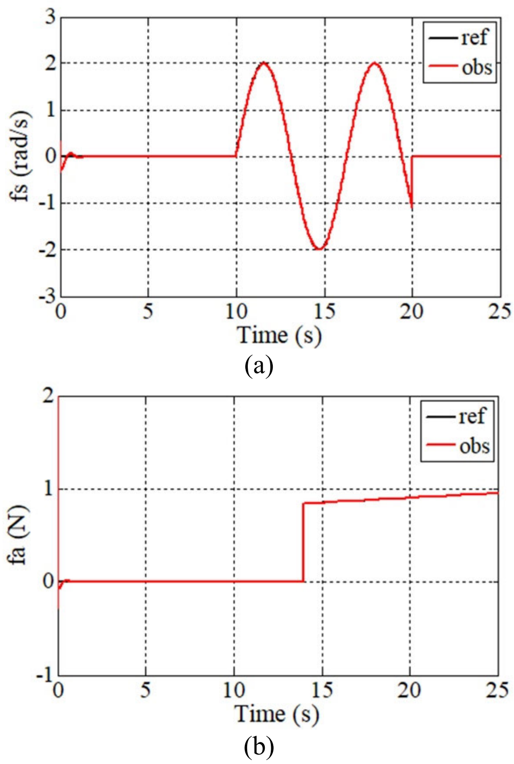

FIGURE 8. Sensor fault $\mathbf{f_s}$, actuator fault $\mathbf{f_a}$, and its estimate. Black dashed lines show the reference signal of faults, red solid lines represent the observed faults. (a) sensor fault $\mathbf{f_s}$ and its estimate. (b) actuator fault $\mathbf{f_a}$ and its estimate.

$$f_a = \begin{cases} 0.15\sin(1.5(t-10)) & 10 \le t < 20 \\ 0, & else \end{cases}$$

To explain the effectiveness of the proposed FTTC approach, comparisons have been made between the proposed method in this article and the proposed one in [45]. By solving the LMI conditions (55) represented in [45], we obtain the observer and tracking control gains as following:

$$\begin{aligned}
L_1^1 &= [104.3249\ 96.1468]\,, \\
L_2^1 &= [134.8041\ 71.4872]\,, \\
L_3^1 &= [115.1214\ 86.3114]\,, \\
L_4^1 &= [126.2125\ 73.5021] \\
L_1^2 &= 85.4412,\ L_2^2 = 88.7540, \\
L_3^2 &= 81.0140,\ L_4^2 = 86.3201 \\
K_1 &= [1.2015 - 0.8143]\,, \\
K_2 &= [1.3325 - 0.7430]\,, \\
K_3 &= [0.9910 - 0.7723]\,, \\
K_4 &= [1.1809 - 0.8137] \\
K_1^f &= 0.0130,\ K_2^f = -0.0083, \\
K_3^f &= 0.0251,\ K_4^f = -0.0061.
\end{aligned}$$

The method in [45] is applied into the faulty system to compare our fault estimation and fault tolerant tracking

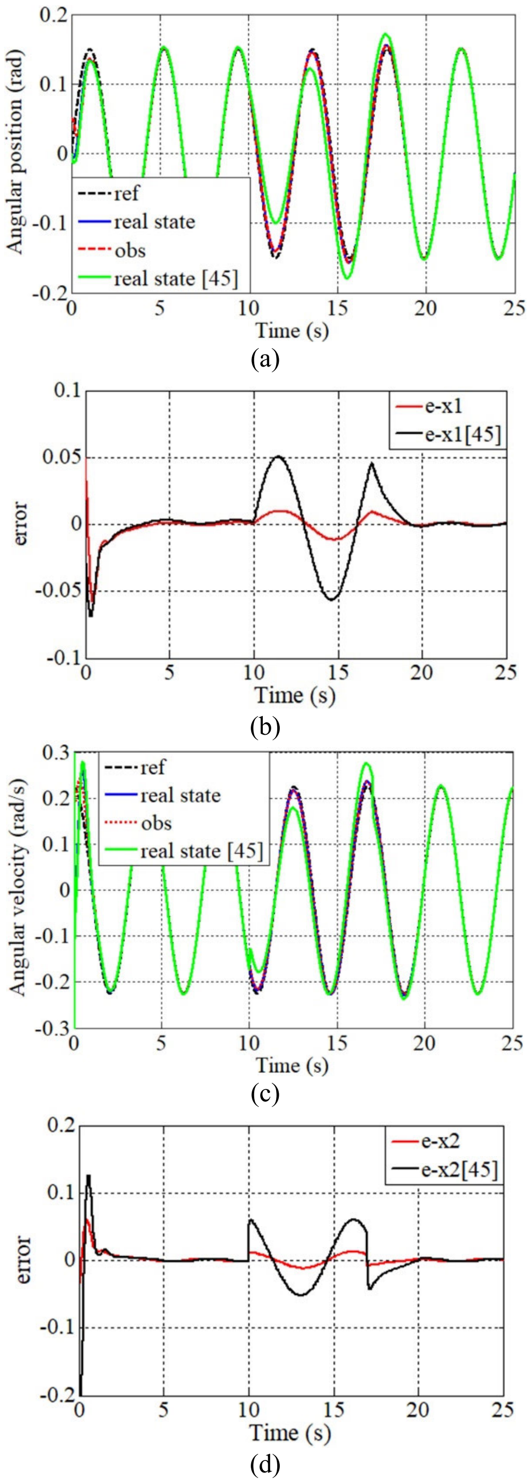

FIGURE 9. Reference states, states of faulty system, estimation and states of [45]. Black dashed lines show the reference signal, blue solid lines represent the real states obtained by the mentioned approach, red dashed lines show the observed states, green solid lines give the real states obtained by the method mentioned in [45]. (a) angular position. (b) error of angular position. (c) angular velocity. (d) error of angular velocity position.

control scheme. The simulation results are shown in Figure 9-Figure12. The comparison results of states tracking are presented in Figure 9. From Figure 9(b) and Figure 9(d), it can

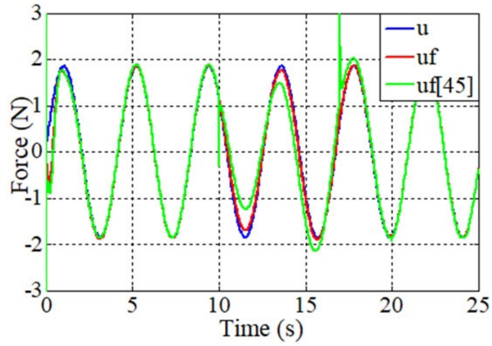

FIGURE 10. Reference, FTC signals and the method in [45]. blue solid line show the control input signal of reference model, red solid line show the control input signal with FTC, green solid line show the control signal of the method in [45].

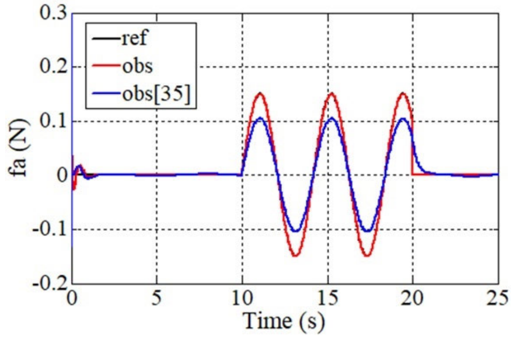

FIGURE 11. The comparison of actuator fault estimation. Black dashed line represent the reference of actuator fault, red solid line show the observed actuator fault obtained by the proposed approach, blue solid line give the observed actuator fault obtained by the approach proposed in [45].

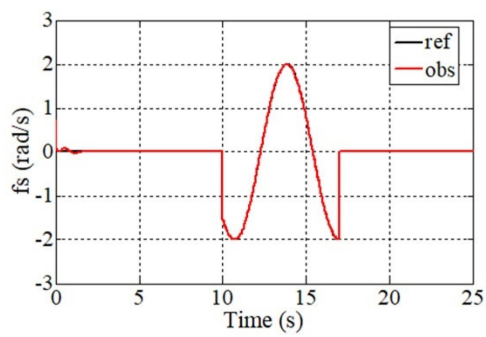

FIGURE 12. Sensor fault f_s and its estimate. Black dashed line represent the reference of sensor fault, red solid line show the observed sensor fault obtained by the proposed method.

be noted that the tracking performance of the states were enhanced by 26% when the faults occurred. The control input of reference model, fault tolerant tracking control signal and the control signal of the method in [45] are illustrated in Figure 10. The comparison of actuator fault estimation is represented in Figure 11. Figure 12 gives the result of the sensor fault f_s and its estimate using our approach.

It is worth pointing out that the performance of FTTC depends on the faults estimate quality. From Figure 9, it is obviously noted that the proposed FTTC method can not only compensate the sensor and actuator faults simultaneously but also achieve good tracking performance of the faulty system.

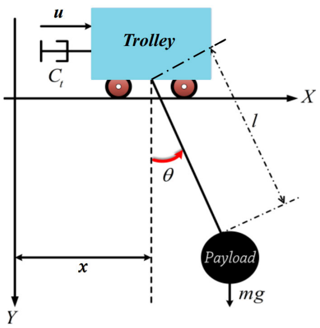

FIGURE 13. The schematics of two-dimensional overhead crane dynamic system.

TABLE 1. MSE comparison of the two controllers in different estimations.

Simulation states	Methods	MSE of error
Angular position	the proposed method	0.00008
	the method in [45]	0.00052
Angular velocity	the proposed method	0.00014
	the method in [45]	0.00051
Actuator fault estimation	the proposed method	0.00293
	the method in [45]	0.00836
Sensor fault estimation	the proposed method	0.00251
	the method in [45]	0.00836

In Figure 11, it is obviously noted that the mentioned fuzzy observer can obtain better estimate quality for the actuator fault signal than the mentioned observer in [45]. Table 1 gives a general overview of the comparison results from the two methods based on MSE. It can be seen that all the MSE of the proposed method are smaller than the observer in [45] in the estimation of unmeasured states and SAFs.

Remark 4: Our objective is to find more relaxed and more accurate results. Therefore, the fault-free system is used as a standard reference model by which the tracking control law is designed. Then, we constructed the novel fuzzy observer to estimate the unmeasured state and SAFs. Moreover, we have obtained a good estimation quality of state and both sensor and actuator fault. Indeed, the fault tolerant control track state to the desired trajectories. As conclusion, we prove the efficiency of our method and we can conclude that our method upgrade the result given in [45]. The tracking problem is addressed with more complex actuator faults such as exponential actuator fault and time varying actuator fault. Whereas, in many researches [38], [39], [40], [41], only the constant actuator fault is studied.

Example 2 (The Overhead Crane System): The dynamical 2-D model of the overhead crane system is shown in Figure 13 [47], the nonlinear dynamic system is represented as follows:

$$\begin{cases} (M+m)\ddot{x} + ml\left(\ddot{\theta}\cos\theta - \dot{\theta}\sin\theta\right) = u - C_t\dot{x} \\ m\ddot{x}\cos\theta + ml\ddot{\theta} + mg\sin\theta = 0 \end{cases}$$

In order to give the state space equations of the overhead crane system, the state vector $\mathbf{x} = [x_1 x_2 x_3 x_4]^T = [x\theta\dot{x}\dot{\theta}]^T$ is selected, u represents control input signal. The state-space expression of the dynamic system is given as the following form:

$$\begin{bmatrix} \dot{x}_1 \\ \dot{x}_2 \\ \dot{x}_3 \\ \dot{x}_4 \end{bmatrix} = \begin{bmatrix} 0 & 0 & 1 & 0 \\ 0 & 0 & 0 & 1 \\ 0 & \frac{mg\cos x_2 \sin x_2}{(M+m\sin^2 x_2)x_2} & \frac{-C_t}{M+m\sin^2 x_2} & \frac{mlx_4\sin x_2}{M+m\sin^2 x_2} \\ 0 & \frac{-(M+m)g\sin x_2}{l(M+m\sin^2 x_2)x_2} & \frac{C_t\cos x_2}{l(M+m\sin^2 x_2)} & \frac{-mx_4\sin x_2\cos x_2}{M+m\sin^2 x_2} \end{bmatrix} + \begin{bmatrix} 0 \\ 0 \\ \frac{1}{M+m\sin^2 x_2} \\ \frac{-\cos x_2}{l(M+m\sin^2 x_2)} \end{bmatrix} u$$

Since actuator fault in the dynamic nonlinear system is an important subject of interest here, we define $F_i = B_i$, $i = 1, \cdots, r$. The common approach is always used to model any change in the system parameters with additive form or any fault which is regarded as an offset in an actuator [48,2]. Moreover, the angle θ in overhead crane system is always small so that the expression $\lim\limits_{t-0} \frac{\sin x_2}{x_2} = 1$ satisfies, the overhead crane system with sensor and actuator faults can be written as:

$$\begin{bmatrix} \dot{x}_{f_1} \\ \dot{x}_{f_2} \\ \dot{x}_{f_3} \\ \dot{x}_{f_4} \end{bmatrix} = \begin{bmatrix} 0 & 0 & 1 & 0 \\ 0 & 0 & 0 & 1 \\ 0 & \frac{mg\cos x_{f_2}}{M+m\sin^2 x_{f_2}} & \frac{-C_t}{M+m\sin^2 x_{f_2}} & \frac{mlx_{f_4}\sin x_{f_2}}{M+m\sin^2 x_{f_2}} \\ 0 & \frac{-(M+m)g}{l(M+m\sin^2 x_{f_2})} & \frac{C_t\cos x_{f_2}}{l(M+m\sin^2 x_{f_2})} & \frac{-mx_4\sin x_{f_2}\cos x_{f_2}}{M+m\sin^2 x_{f_2}} \end{bmatrix} \begin{bmatrix} x_{f_1} \\ x_{f_2} \\ x_{f_3} \\ x_{f_4} \end{bmatrix} + \begin{bmatrix} 0 \\ 0 \\ \frac{1}{M+m\sin^2 x_{f_2}} \\ \frac{-\cos x_{f_2}}{l(M+m\sin^2 x_{f_2})} \end{bmatrix} (u + f_a)$$

$$y_f = \begin{bmatrix} 1 & 0 & 0 & 0 \\ 0 & 1 & 0 & 0 \\ 0 & 0 & 1 & 0 \\ 0 & 0 & 0 & 1 \end{bmatrix} \begin{bmatrix} x_{f_1} \\ x_{f_2} \\ x_{f_3} \\ x_{f_4} \end{bmatrix} + \begin{bmatrix} 0 \\ 0 \\ 0 \\ 1 \end{bmatrix} f_s \tag{35}$$

Similarly with example 1, to meet the situations of practical application, the same crane parameters are chosen as [47]: $M = 10\text{kg}, m = 4\text{kg}, l = 0.5\text{m}, C_t = 0.1\text{Ns/m}$, and $g = 9.8\text{m/s}^2$.

The same crane parameters are chosen as [47]: $M = 10\text{kg}, m = 4\text{kg}, l = 0.5\text{m}, C_t = 0.1\text{Ns/m}$, and $g = 9.8\text{m/s}^2$. The payload angle position is chosen as: $-\pi/12 \leq$

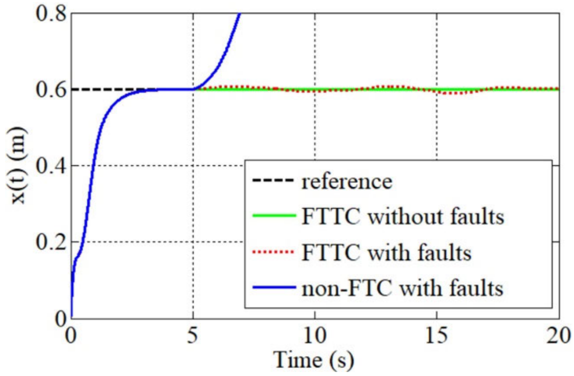

(a)

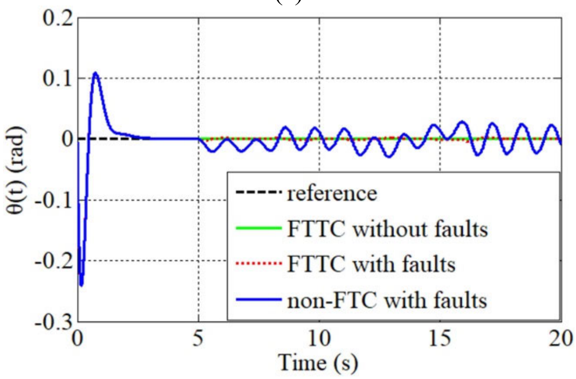

(b)

FIGURE 14. Results of the overhead crane system applied FTTC without faults, FTTC with faults and non-FTC with faults, respectively. Black dashed lines show the desired signal, green solid lines represent the real states obtained by FTTC without faults, red dashed lines give the observed state obtained by FTTC with faults, blue solid lines represent the real state by non-FTC with faults. (a) position. (b) swing angle.

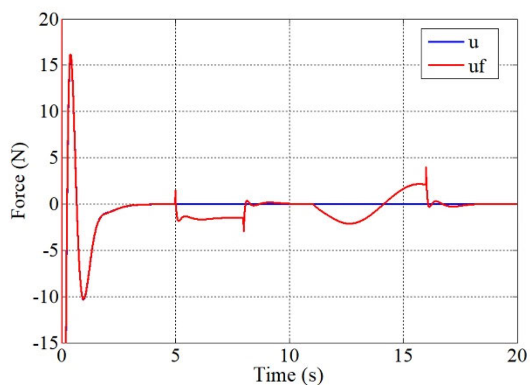

FIGURE 15. FTTC control signals with faults and FTTC control signals without faults. Blue solid line show the control input signal of FTTC control signals with faults, red solid line show the control input signal of FTTC control signals without faults.

$\theta(t) \leq \pi/12$, and the angle velocity is chosen as: $-\pi/4 \leq \dot{\theta}(t) \leq \pi/4$. Furthermore, $\xi_1(t) = \frac{1}{M+m\sin x_2}$, $\xi_2(t) = cosx_2$, $\xi_3(t) = x_4\sin x_2$ are premise variables; also, $\xi_{1,max} = 1/M$, $\xi_{1,min} = 1/(M + m\sin^2(\pi/12)$, $\xi_{2,max} = 1$, $\xi_{2,min} = \cos(\pi/12)$, $\xi_{3,max} = \frac{\pi}{4}\sin(\pi/12)$, $\xi_{3,min} = -\frac{\pi}{4}\sin(\pi/12)$. Therefore, the Eq. (35) is rewritten as:

Rule i: if $\xi_1(t)$ is$F_{1i}$and$\xi_2(t)$ is$F_{2i}$and$\xi_3(t)$ isF_{3i} then

$$\begin{cases} \dot{x}_f(t) = \bar{A}_i x_f(t) + \bar{B}_i(u_f(t) + f_a(t)) \\ y_f(t) = \bar{D}_i x_f(t) + E_i f_s(t) \end{cases} \quad \text{for } i = 1, \cdots, 8.$$

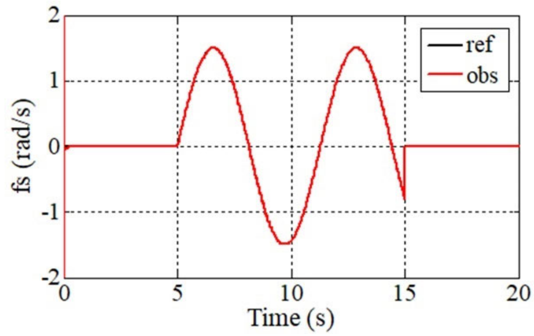

(a)

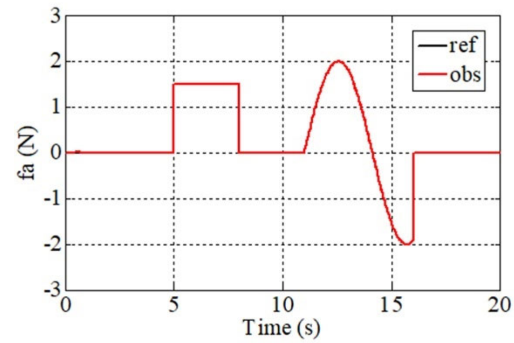

(b)

FIGURE 16. Sensor fault fs, actuator fault fa, and its estimate. Black dashed lines show reference signal of faults, red solid lines represent the observed faults. (a) sensor fault fs and its estimate. (b) actuator fault fa and its estimate.

where

$$\bar{A}_i = \begin{bmatrix} 0 & 0 & 1 & 0 \\ 0 & 0 & 0 & 1 \\ 0 & mg\xi_2\xi_1 & -C_t\xi_1 & ml\xi_3\xi_1 \\ 0 & \frac{-(M+m)g\xi_1}{l} & \frac{C_t\xi_2\xi_1}{l} & -m\xi_3\xi_2\xi_1 \end{bmatrix},$$

$$\bar{B}_i = \begin{bmatrix} 0 \\ 0 \\ \xi_1 \\ \frac{-\xi_2\xi_1}{l} \end{bmatrix}, \bar{D}_i = \begin{bmatrix} 1 & 0 & 0 & 0 \\ 0 & 1 & 0 & 0 \\ 0 & 0 & 1 & 0 \\ 0 & 0 & 0 & 1 \end{bmatrix}, E_i = \begin{bmatrix} 0 \\ 0 \\ 0 \\ 1 \end{bmatrix}$$

Uncertain matrix is chosen as: $H = [000.20.5]^T$, $E_a = [0\ 2\ 0\ 0]$, $\tilde{H} = \check{H} = [000.20.50000]^T$,

$$\tilde{E}_a = \check{E}_a = [0\ 2\ 0\ 0\ 0\ 0\ 0\ 0].$$

The SAFs are chosen as:

$$f_s = \begin{cases} 1.5\sin(t-10) & 5 \leq t < 15 \\ 0 & else \end{cases}$$

$$f_a = \begin{cases} 1.5 & 5 \leq t < 8 \\ 2\sin(t-11) & 11 \leq t < 16 \\ 0 & else \end{cases}$$

In the fault free case, we choose the parameter as: $Q = 10^{-2} \times I_{4\times4}$, $\alpha_1 = 0.1$, we can obtain the feedback gains K_{h_i} for $i = 1, 2, 3, 4$ by solving the LMIs conditions given in Theorem 1. For the purpose of the design of the fuzzy faults and states observer according to Theorem 2, we choose the design parameters as $Q_1 = 10^{-2} \times I_{8\times8}$, $Q_2 = Q_3 = 10^{-2}$,

$\alpha_2 = 1$. then, by solving the LMIs conditions in Theorem 2, the observer gains L_i, L_{fa_i}, L_{fs_i} for $i = 1, \cdots, 8$ can be obtained. In Theorem 3, we chosen the parameters as: $\alpha_3 = \alpha_4 = 0.01$, $\beta_1 = \beta_2 = \beta_3 = 10$. Then, the control gains K_{PI_i} for $i = 1, 2, 3, 4$ can be computed.

Besides, the initial system states $x(0) = \hat{x}(0) = [0\ 0\ 0\ 0]$ and the reference trajectory $x_d(t) = [0.6\ 0\ 0\ 0]$ are used.

Aiming to evaluate the proposed method, the comparison was carried out to illustrate the effectiveness of the proposed control method. Now, comparison was provided in three different cases: 1) the FTTC method was utilized without any sensor and actuator faults; 2) the FTTC method was utilized with sensor and actuator faults; 3) non- FTTC method was used when sensor and actuator faults happened.

Figure 14. and Figure 16. represent the performance of the proposed FTTC method. From Figure 14, it is observed that the trolley is driven from the initial point to the desired position with satisfied tracking performance when no faults occur. However, when we have applied the faults but no FTC in the system, the position of the trolley can not converge to the desired point and the big angle oscillation occurs. By comparison, the proposed FTTC method can compensate the faults effectively and ensure the better tracking performance between the reference signal and the states of faulty system. It can be obviously seen that, despite the existence of faults and uncertainty, the degradation of tracking control performance is not remarkable since the faults applied in the system are well estimated and compensated by the proposed FTTC method. The control input of FTTC control signals with faults and FTTC control signals without faults are illustrated in Figure 15.The considered fault signals and their estimate are given in Figure 16.

Remark 5: Theoretically, it should be noted that any type of bounded sensor and actuator faults can be attenuated by the proposed method in Example 1 and Example 2. The design parameter values, such as attenuation coefficient γ, should be chosen properly to deal with larger faults.

V. CONCLUSION

In this paper, a new fuzzy observer-based FD and FTTC approach have been proposed for a T-S fuzzy uncertain system affected by SAFs. The mentioned observer can estimate unmeasurable states and SAFs of the faulty system simultaneously. Meanwhile, the developed PI-type control law achieves satisfactory control performance including the stability and tracking issue in spite the presence of faults and uncertainties. The fault diagnosis and tracking conditions are formulated in terms of LMIs using an appropriate Lyapunov function. For investigating the advantage of the proposed FTTC method, it is used to control an Inverted Pendulum system and an Overhead Crane system. Simulation results show that the stability and favorable tracking performance can be achieved by using the proposed FTTC method. The results presented that the tracking performance was enhanced by 23% compared with the method in [45] when the faults occurred in Case 3 of Example 1. The estimation error of SAFs in all cases were not exceed 2% at the steady stage when the proposed method was utilized. It is important to extend the proposed FTTC method to the fuzzy uncertain nonlinear systems affected by time-delay and disturbances and try other observers to obatian better performance in diferenct cases, such as: adaptive adjustable dimension observer [49] and integrated observer [50], which would be considered as the further work.

REFERENCES

[1] F.-J. Lin, I.-F. Sun, K.-J. Yang, and J.-K. Chang, "Recurrent fuzzy neural cerebellar model articulation network fault-tolerant control of six-phase permanent magnet synchronous motor position servo drive," *IEEE Trans. Fuzzy Syst.*, vol. 24, no. 1, pp. 153–167, Feb. 2016.

[2] J. Lan and R. J. Patton, "A new strategy for integration of fault estimation within fault-tolerant control," *Automatica*, vol. 69, pp. 48–59, Jul. 2016.

[3] Y. Li, K. Sun, and S. Tong, "Adaptive fuzzy robust fault-tolerant optimal control for nonlinear large-scale systems," *IEEE Trans. Fuzzy Syst.*, vol. 26, no. 5, pp. 2899–2914, Oct. 2018.

[4] Q.-Y. Fan and G.-H. Yang, "Event-based fuzzy adaptive fault-tolerant control for a class of nonlinear systems," *IEEE Trans. Fuzzy Syst.*, vol. 26, no. 5, pp. 2686–2698, Oct. 2018.

[5] Y.-H. Jing and G.-H. Yang, "Fuzzy adaptive fault-tolerant control for uncertain nonlinear systems with unknown dead-zone and unmodeled dynamics," *IEEE Trans. Fuzzy Syst.*, vol. 27, no. 12, pp. 2265–2278, Dec. 2019.

[6] X.-G. Guo, X. Fan, and C. K. Ahn, "Adaptive event-triggered fault detection for interval type-2 T–S fuzzy systems with sensor saturation," *IEEE Trans. Fuzzy Syst.*, vol. 29, no. 8, pp. 2310–2321, Aug. 2021.

[7] Z. Ruan, Q. Yang, S. S. Ge, and Y. Sun, "Adaptive fuzzy fault tolerant control of uncertain MIMO nonlinear systems with output constraints and unknown control directions," *IEEE Trans. Fuzzy Syst.*, vol. 30, no. 5, pp. 1224–1238, May 2022.

[8] J. Gong, Y. Ma, B. Jiang, and Z. Mao, "Distributed adaptive fault-tolerant formation control for heterogeneous multiagent systems under switching directed topologies," *J. Franklin Inst.*, vol. 359, no. 8, pp. 3366–3388, May 2022.

[9] Y. Ren, A. Wang, and H. Wang, "Fault diagnosis and tolerant control for discrete stochastic distribution collaborative control systems," *IEEE Trans. Syst. Man, Cybern. Syst.*, vol. 45, no. 3, pp. 462–471, Mar. 2015.

[10] L. Yao, J. Qin, H. Wang, and B. Jiang, "Design of new fault diagnosis and fault tolerant control scheme for non-Gaussian singular stochastic distribution systems," *Automatica*, vol. 48, no. 9, pp. 2305–2313, Sep. 2012.

[11] L. Guo and H. Wang, "Fault detection and diagnosis for general stochastic systems using B-spline expansions and nonlinear filters," *IEEE Trans. Circuits Syst. I, Reg. Papers*, vol. 52, no. 8, pp. 1644–1652, Aug. 2005.

[12] T. Li and Y. Zhang, "Fault detection and diagnosis for stochastic systems via output PDFs," *J. Franklin Inst.*, vol. 348, no. 6, pp. 1140–1152, Aug. 2011.

[13] D. Qiao and Y. Wang, "Fault-tolerant control for linear parameter varying systems with integral measurements based on event-triggered mechanism," *J. Franklin Inst.*, vol. 358, no. 16, pp. 8250–8269, Oct. 2021.

[14] M. Liu and P. Shi, "Sensor fault estimation and tolerant control for itô stochastic systems with a descriptor sliding mode approach," *Automatica*, vol. 49, no. 5, pp. 1242–1250, May 2013.

[15] Z. Qiao, T. Shi, Y. Wang, Y. Yan, C. Xia, and X. He, "New sliding-mode observer for position sensorless control of permanent-magnet synchronous motor," *IEEE Trans. Ind. Electron.*, vol. 60, no. 2, pp. 710–719, Feb. 2013.

[16] S. Makni, M. Bouattour, A. E. Hajjaji, and M. Chaabane, "H_/H_∞ observer design for nonlinear T–S fuzzy systems subject to sensor and actuator faults," in *Proc. 18th Int. Conf. Sci. Techn. Autom. Control Comput. Eng. (STA)*, Dec. 2017, pp. 296–301.

[17] Y. Lu and Y. Song, "Descriptor observer based approach for adaptive reconstruction of measurement noises and sensor faults in uncertain nonlinear systems," in *Proc. 27th Chin. Control Decis. Conf. (CCDC)*, May 2015, pp. 2764–2769.

[18] M. Bouattour, M. Chadli, A. El Hajjaji, and M. Chaabane, "Estimation of state, actuator and sensor faults for T-S models," in *Proc. 49th IEEE Conf. Decis. Control (CDC)*, Dec. 2010, pp. 1613–1618.

[19] K. Tanaka, H. Ohtake, and H. O. Wang, "A descriptor system approach to fuzzy control system design via fuzzy Lyapunov functions," *IEEE Trans. Fuzzy Syst.*, vol. 15, no. 3, pp. 333–341, Jun. 2007.

[20] M. Hashemi, A. K. Egoli, M. Naraghi, and C. P. Tan, "Saturated fault tolerant control based on partially decoupled unknown-input observer: A new integrated design strategy," *IET Control Theory Appl.*, vol. 13, no. 13, pp. 2104–2113, Sep. 2019.

[21] M. Hashemi and C. P. Tan, "Integrated fault estimation and fault tolerant control for systems with generalized sector input nonlinearity," *Automatica*, vol. 119, Sep. 2020, Art. no. 109098.

[22] J. Lan, R. J. Patton, and X. Zhu, "Integrated fault-tolerant control for a 3-DOF helicopter with actuator faults and saturation," *IET Control Theory Appl.*, vol. 11, no. 14, pp. 2232–2241, Sep. 2017.

[23] I. Zare, P. Setoodeh, and M. H. Asemani, "Fault-tolerant tracking control of discrete-time T–S fuzzy systems with input constraint," *IEEE Trans. Fuzzy Syst.*, vol. 30, no. 6, pp. 1914–1928, Jun. 2022.

[24] J. Qin, Q. Ma, H. Gao, and W. X. Zheng, "Fault-tolerant cooperative tracking control via integral sliding mode control technique," *IEEE/ASME Trans. Mechatronics*, vol. 23, no. 1, pp. 342–351, Feb. 2018.

[25] S. Abdelmalek, L. Barazane, and A. Larabi, "An advanced robust fault-tolerant tracking control for a doubly fed induction generator with actuator faults," *TURKISH J. Electr. Eng. Comput. Sci.*, vol. 25, pp. 1346–1357, 2017.

[26] M. Bataghva and M. Hashemi, "Adaptive sliding mode synchronisation for fractional-order non-linear systems in the presence of time-varying actuator faults," *IET Control Theory Appl.*, vol. 12, no. 3, pp. 377–383, Feb. 2018.

[27] H. Dou, "Adaptive robust fault-tolerant control for a two-slider synchronization system with a flexible beam," *J. Franklin Inst.*, vol. 358, no. 18, pp. 9561–9586, Dec. 2021.

[28] Y. Xiong and M. Saif, "Unknown disturbance inputs estimation based on a state functional observer design," *Automatica*, vol. 39, no. 8, pp. 1389–1398, Aug. 2003.

[29] T. Lee, C. Peng, and L. Saeid, "Observer-based H_∞ fault-tolerant control for linear systems with sensor and actuator faults," *IEEE Syst. J.*, vol. 13, no. 2, pp. 1981–1989, Jun. 2019.

[30] C. Zhang and I. M. Jaimoukha, "Fault-tolerant controller design with a tolerance measure for systems with actuator and sensor faults," in *Proc. Amer. Control Conf. (ACC)*, May 2017, pp. 4129–4134.

[31] N. Xu, L. Chen, R. Yang, and Y. Zhu, "Multi-controller-based fault tolerant control for systems with actuator and sensor failures: Application to 2-body point absorber wave energy converter," *J. Franklin Inst.*, vol. 359, no. 12, pp. 5919–5934, Aug. 2022.

[32] H. Wang, Y. Kang, L. Yao, H. Wang, and Z. Gao, "Fault diagnosis and fault tolerant control for T–S fuzzy stochastic distribution systems subject to sensor and actuator faults," *IEEE Trans. Fuzzy Syst.*, vol. 29, no. 11, pp. 3561–3569, Nov. 2021.

[33] S. K. Kommuri, M. Defoort, H. R. Karimi, and K. C. Veluvolu, "A robust observer-based sensor fault-tolerant control for PMSM in electric vehicles," *IEEE Trans. Ind. Electron.*, vol. 63, no. 12, pp. 7671–7681, Dec. 2016.

[34] S. Aouaouda, M. Chadli, M. Boukhnifer, and H. R. Karimi, "Robust fault tolerant tracking controller design for vehicle dynamics: A descriptor approach," *Mechatronics*, vol. 30, pp. 316–326, Sep. 2015.

[35] L. Wang, J. Song, R. Zhang, and F. Gao, "Constrained model predictive fault-tolerant control for multi-time-delayed batch processes with disturbances: A Lyapunov–Razumikhin function method," *J. Franklin Inst.*, vol. 358, no. 18, pp. 9483–9509, Dec. 2021.

[36] M. Bataghva and M. Hashemi, "Adaptive sliding mode synchronisation for fractional-order non-linear systems in the presence of time-varying actuator faults," *IET Control Theory Appl.*, vol. 16, no. 9, pp. 377–383, Jun. 2018.

[37] Y.-C. Chang, C.-H. Chen, Z.-C. Zhu, and Y.-W. Huang, "Speed control of the surface-mounted permanent-magnet synchronous motor based on Takagi–Sugeno fuzzy models," *IEEE Trans. Power Electron.*, vol. 31, no. 9, pp. 6504–6510, Sep. 2016.

[38] T. Bouarar, B. Marx, D. Maquin, and J. Ragot, "Trajectory tracking fault tolerant controller design for Takagi–Sugeno systems subject to actuator faults," in *Proc. Int. Conf. Commun., Comput. Control Appl. (CCCA)*, Mar. 2011, pp. 1–6.

[39] M. Bouattour, M. Chadli, A. E. Hajjaji, and M. Chaabane, "State and faults estimation for T-S models and application to fault diagnosis," *IFAC Proc. Volumes*, vol. 42, no. 8, pp. 492–497, 2009.

[40] Z. Gao and H. Wang, "Descriptor observer approaches for multivariable systems with measurement noises and application in fault detection and diagnosis," *Syst. Control Lett.*, vol. 55, no. 4, pp. 304–313, Apr. 2006.

[41] D. Ichalal, B. Marx, J. Ragot, and D. Maquin, "New fault tolerant control strategies for nonlinear Takagi–Sugeno systems," *Int. J. Appl. Math. Comput. Sci.*, vol. 22, no. 1, pp. 197–210, Mar. 2012.

[42] C. Li, X. Pan, and G. Wang, "Torque tracking control of electric load simulator with active motion disturbance and nonlinearity based on T–S fuzzy model," *Asian J. Control*, vol. 22, no. 3, pp. 1280–1294, May 2020.

[43] C. C. Li, Y. F. Li, and G. L. Wang, "H_∞ output tracking control of uncertain and disturbed nonlinear systems based on neural network model," *Int. J. Syst. Sci.*, vol. 48, no. 10, pp. 2091–2103, Sep. 2017.

[44] G. Li, T. Li, and Q. Zhao, "Fault tolerant shape control for particulate process systems under simultaneous actuator and sensor faults," *IET Control Theory Appl.*, vol. 11, no. 15, pp. 2448–2457, Oct. 2017.

[45] T. Bouarar, B. Marx, D. Maquin, and J. Ragot, "Fault-tolerant control design for uncertain Takagi–Sugeno systems by trajectory tracking: A descriptor approach," *IET Control Theory Appl.*, vol. 7, no. 14, pp. 1793–1805, Sep. 2013.

[46] B. Mansouri, N. Manamanni, K. Guelton, A. Kruszewski, and T. Guerra, "Output feedback LMI tracking control conditions with H_∞ criterion for uncertain and disturbed T–S models," *Inf. Sci.*, vol. 179, pp. 446–457, Oct. 2008.

[47] C. Li, Y. Xia, and W. Wang, "H_∞ output-feedback anti-swing control for a nonlinear overhead crane system with disturbances based on T-S fuzzy model," *IEEE Access*, vol. 9, pp. 135571–135584, 2021.

[48] M. Hashemi, A. K. Egoli, and M. Naraghi, "Integrated fault tolerant control for saturated systems with additive faults: A comparative study of saturation models," *Int. J. Control, Autom. Syst.*, vol. 17, no. 4, pp. 1019–1030, Apr. 2019.

[49] X. Liu, J. Han, X. Wei, H. Zhang, and X. Hu, "Distributed fault detection for non-linear multi-agent systems: An adjustable dimension observer design method," *IET Control Theory Appl.*, vol. 13, no. 15, pp. 2407–2415, Aug. 2019.

[50] J. Li, S. Huang, "Distributed fault detection for non-linear multi-agent systems: An adjustable dimension observer design method," *Int. J. Robust Nonlinear Control.*, vol. 30, no. 14, pp. 5678–5692, Sep. 2020.

CHENGCHENG LI received the B.S. degree in mechatronics engineering from Central South University, Changsha, China, and the M.S. and Ph.D. degrees in mechatronics engineering from the Harbin Institute of Technology, Harbin, China.

Currently, he is an Associate Professor of automatic control with Lanzhou Jiaotong University, Lanzhou, China. His current research interests include robust control and filtering and analysis and control of nonlinear systems.

YUXIANG XIA received the B.S. and M.S. degrees in mechatronics engineering from the Harbin University of Commerce, Harbin, China.

She has been a Lecturer of automatic control with Lanzhou Jiaotong University, Lanzhou, China. Her current research interests include process automation, the control of nonlinear systems, intelligent control, and optimal control.